

Perturbation-Robust Predictive Modeling of Social Effects by Network Subspace Generalized Linear Models

Jianxiang Wang^a, Can M. Le^b, and Tianxi Li^c

^aRutgers University – New Brunswick

^bUniversity of California, Davis

^cUniversity of Minnesota, Twin Cities

October 4, 2024

Abstract

Network-linked data, where multivariate observations are interconnected by a network, are becoming increasingly prevalent in fields such as sociology and biology. These data often exhibit inherent noise and complex relational structures, complicating conventional modeling and statistical inference. Motivated by empirical challenges in analyzing such data sets, this paper introduces a family of network subspace generalized linear models designed for analyzing noisy, network-linked data. We propose a model inference method based on subspace-constrained maximum likelihood, which emphasizes flexibility in capturing network effects and provides a robust inference framework against network perturbations. We establish the asymptotic distributions of the estimators under network perturbations, demonstrating the method's accuracy through extensive simulations involving random network models and deep-learning-based embedding algorithms. The proposed methodology is applied to a comprehensive analysis of a large-scale study on school conflicts, where it identifies significant social effects, offering meaningful and interpretable insights into student behaviors.

1 Introduction

Network data analysis has become increasingly popular due to its wide-ranging applications in the social sciences [Holme, 2015, Van den Bos et al., 2018], biological sciences [Özgür et al., 2008, Zeng et al., 2018], and engineering [Le Gat, 2014, Cuadra et al., 2015]. A notable category of social network data concerns network-linked objects, where the interactions or relationships among individuals are depicted through network structures, and each individual typically has associated response variables and covariates. Such structures are frequently encountered in studies examining social influences on human behavior [Michell and West, 1996, Michell, 2000, Harris, 2009, Paluck et al., 2016]. In this paper, we focus on analyzing student behavior in the context of school conflicts, using the data from Paluck et al. [2016]. Despite the development of numerous statistical models to analyze network-linked data in recent years [Zhang et al., 2016, Li et al., 2019, Su et al., 2019, Zhang et al., 2020, Sit and Ying, 2021, Mao et al., 2021, Mukherjee et al., 2021, Le and Li, 2022, Hayes et al., 2022, Fang et al., 2023, He et al., 2023, Lunde et al., 2023, Zhu et al., 2017, Wu and Leng, 2023, Armillotta and Fokianos, 2023, Chang and Paul, 2024], the noisy nature of the network structures in this study necessitates non-trivial generalizations of the existing literature to effectively analyze the school conflict data. This challenge motivates the development of our new

model. In the following sections, we introduce the school conflict study and review the current literature on predictive modeling for network-linked data.

1.1 Social effect analysis in the school conflicts study

A prospective study by [Paluck et al. \[2016\]](#) investigated the effects of randomized anti-conflict interventions on social norms across 56 high schools in New Jersey. In the treatment schools, students were randomly selected to participate in educational workshops on school conflicts. Data collection included official records from school administrations and student questionnaires, where students provided personal information, opinions on conflict-related events, and a list of their closest friends at both the beginning and end of the school year, allowing for the mapping of social networks within each school. In 25 of these schools, which were randomly selected from the 56, the experimenters introduced educational workshops aimed at a small group of students to reduce school conflicts. The field experiment sought to demonstrate that introducing educational interventions to students could help mitigate conflicts within schools. The anti-conflict impact was measured through the allocation of orange wristbands, which rewarded students for friendly or conflict-mitigating actions.

In this study, a key object of interest is the social influence, which could play a significant role in disseminating the effects of the intervention throughout the entire school. To facilitate the analysis of social influence, the experimenters recorded friendship relations in terms of “how much time two students spend together.” In addition to social influence, the study aims to understand the impact of various background covariates, such as gender, race, and family conditions. While the original study by [Paluck et al. \[2016\]](#) utilized social relations to infer social effects, recent work by [Le and Li \[2022\]](#) highlighted the importance of accounting for noisy observations in friendship relations to ensure valid inference. Specifically, two waves of surveys were administered within the same school year to capture social relations. However, the overlap between the two waves was limited. Figure 1 displays the edge overlap proportions across the 25 schools, showing that, in most schools, only about 50% of the edges overlapped between the two periods. Such high levels of noise in the observations can jeopardize the validity of statistical inference if the network structure errors are not adequately addressed in the analysis.

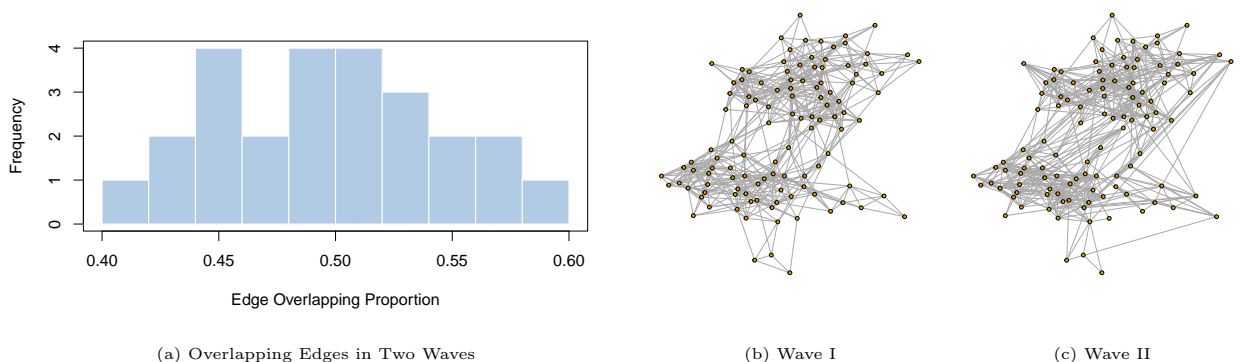


Figure 1: Left panel: the proportion of overlapping edges in two waves in the study, across 25 schools. Right panel: the networks in two waves in one example school.

More generally, noisy observations of network structures are frequently encountered in other empirical studies, particularly in the social sciences [[Onnela et al., 2007](#), [Yu et al., 2008](#), [Harris, 2009](#)]. Furthermore, popular graph-embedding methods in machine learning [[Perozzi et al., 2014](#), [Grover and Leskovec, 2016](#), [Rozemberczki and Sarkar, 2018](#)], which are commonly used to manage network

data in modeling tasks, may introduce additional perturbations due to their inherent randomness. These challenges underscore the need for a general predictive modeling strategy that can account for network perturbations while ensuring validity in inference. Addressing this issue is the central focus of our model development in this paper.

1.2 Predictive models for network-linked data

We focus on predictive modeling for a node-level response variable. Among the available works in literature, relevant predictive models can be categorized into three main classes based on their design. The first class treats the network as a generalized spatial relationship and employs a graph-based autoregressive model to capture dependencies [Zhu et al., 2017, Armillotta and Fokianos, 2023, Wu and Leng, 2023, Chang and Paul, 2024]. The second class of methods incorporates network information through a distance-based dependence structure, assuming that responses are independent if the distance between them exceeds a certain threshold [Su et al., 2019, Sit and Ying, 2021, Mukherjee et al., 2021]. Both of these classes rely on parametric forms of network effects and assume that the observed networks are accurate. While these methods provide informative model inference if the assumed network effect is appropriate, they may lead to misleading conclusions when the assumed parametric form is violated. Additionally, they tend to be vulnerable to errors in the observed network structure, which is a key issue in our motivating application.

The third class of methods employs nonparametric components to model network effects. For instance, Li et al. [2019] introduces the *regression with network cohesion* (RNC) approach, which includes an individual node effects component along with a network smoothing penalty. This method has proven to be flexible for modeling network-linked responses and is applicable to various settings, such as generalized linear models. However, this approach lacks a formal statistical inference framework. A more recent model in this category is the *subspace linear regression* proposed by Le and Li [2022]. Instead of assuming a smooth network effect, this model posits a latent subspace for the network effect. It offers a valid inference framework and demonstrates robustness against network perturbations. However, the model fitting relies on a sequence of geometric projections, which are valid only for linear regression. This restriction can be limiting in practice, as categorical and discrete responses are common in social science applications, such as our motivating example of the school conflict study. In a separately line, Hayes et al. [2022] introduced a model in a similar flavor to to analyze network-mediated effect in causal problems, in which the network effect is parameterized by linear combination of latent vectors. This method can handle other types of response variables, but the latent vectors are assumed to follow the random dot product graph model [Athreya et al., 2018].

In this paper, we build upon the concept of subspace linear regression by introducing a new class of models called *network-subspace generalized linear models* for network-linked data. Our model assumes that the predictive structure lies in the Minkowski sum of the column space of covariates and a latent subspace representing network relationships. We fit the model and conduct inference using subspace-constrained maximum likelihood, demonstrating that valid asymptotic statistical inference is guaranteed under essentially the same level of network perturbation as in the linear regression framework of Le and Li [2022]. This advancement greatly expands the scope of robust predictive modeling and inference for network-linked data, accommodating both categorical and discrete response variables. Notably, the validity of our inference does not depend on a specific network perturbation model, allowing for application in a variety of settings with noisy network data.

We not only validate the inference of our model under traditional random network perturbations

[Bickel and Chen, 2009], but also explore the integration of network effects through modern deep-learning-based embedding techniques commonly used in graph mining. Specifically, for the former, we show the effectiveness of our model for both low-rank and full-rank random network models. For the latter, we investigate three popular methods — DeepWalk [Perozzi et al., 2014], Node2Vec [Grover and Leskovec, 2016], and Diff2Vec [Rozemberczki and Sarkar, 2018]—demonstrating that the inherent noise and perturbations introduced by these algorithms are effectively managed by our model, ensuring accurate inference. Our work thus bridges the gap between rigorous statistical inference and general unsupervised strategies for incorporating network information.

2 Methodology

2.1 Notations

Throughout the paper, we use $c, C > 0$ to denote absolute constants, the values of which may change from line to line. For two sequences of positive scalars $\{a_n\}_{n=1}^\infty$ and $\{b_n\}_{n=1}^\infty$, we write $a_n = o(b_n)$ and $a_n = O(b_n)$ if a_n/b_n converges to zero and a_n/b_n is bounded, respectively. Similarly, for a sequence of random variables $\{X_n\}_{n=1}^\infty$, we write $X_n = o_p(b_n)$ and $X_n = O_p(b_n)$ if X_n/b_n converges to zero and is bounded in probability, respectively. We use $I_n \in \mathbb{R}^{n \times n}$ to denote the identity matrix of size n . For a matrix $A = (A_{ij}) \in \mathbb{R}^{n \times n}$, $\text{tr}(A) = \sum_{i=1}^n A_{ii}$ is the trace, while $\lambda_{\min}(A)$ and $\lambda_{\max}(A)$ are the minimum and maximum eigenvalues of A , respectively, when A is symmetric. For a vector u , $\|u\|$ is the Euclidean norm. For a matrix $W = (W_{ij}) \in \mathbb{R}^{m \times n}$ with $1 \leq n \leq m$ and the singular decomposition $W = \sum_{i=1}^n \sigma_i u_i v_i^\top$, $\|W\| = \max_{1 \leq i \leq n} \sigma_i$, $\|W\|_F = (\sum_{i=1}^n \sigma_i^2)^{1/2}$ and $\|W\|_\infty = \max_{1 \leq i \leq n} \sum_{j=1}^n |W_{ij}|$ represent the spectral norm, the Frobenius norm, and the infinity norm of A , respectively. In addition, W_i is the i -th column of W , and $W_{u:v}$ is the sub-matrix of W with column vectors W_i for $u \leq i \leq v$. We further use $W_{i,u:v}$ to denote the i -th row of $W_{u:v}$.

2.2 Model

We assume there exists a true unobserved relational matrix $P \in \mathbb{R}^{n \times n}$, where P_{ij} describes the strength of the relationship between the nodes i and j . Let $\hat{P} = (\hat{P}_{ij}) \in \mathbb{R}^{n \times n}$ be an approximate relational matrix, which can be viewed as a noisy version of P that is computable from observed relations between observations. An example of this relational model appears in random network modeling literature assumes that the entries of \hat{P} are the observed adjacency connections between nodes, generated as independent Bernoulli random variables with $P = \mathbb{E}[\hat{P}]$, or some improved estimators based on certain statistical estimation methods [Li and Le, 2023]; another example discussed in detail in Section 4.2 involves stochastic embedding algorithms for which \hat{P} is the similarity between the random embedding output. Intuitively, we expect that \hat{P} does not significantly deviate from P .

In addition to the relational matrix \hat{P} , for each node i , we observe (x_i, y_i) , where $x_i \in \mathbb{R}^p$ is a covariate vector and $y_i \in \mathbb{R}$ is a scalar response. Denote by $Y = (y_1, \dots, y_n)^\top \in \mathbb{R}^n$ the response vector and by $X = (x_1, \dots, x_n)^\top \in \mathbb{R}^{n \times p}$ the design matrix.

Conditioning on X and P , we assume that y_1, \dots, y_n are independent random variables drawn from a *generalized linear model* (GLM). Following McCullagh [2019], the probability density or probability mass function of y_i can be expressed in the following form:

$$f(y; \psi_i, \phi) = \exp \left(\frac{y\psi_i - b(\psi_i)}{a(\phi)} + d(y, \phi) \right), \quad i = 1, \dots, n. \quad (1)$$

Here, a , b , and d are specific functions depending on the distribution of y_i . For example, when

$a(\phi) = 1$, $b(\psi_i) = \log(1 + e^{\psi_i})$, and $d(y, \phi) = 0$, (1) leads to a logistic regression; when $a(\phi) = 1$, $b(\psi_i) = e^{\psi_i}$, and $d(y, \phi) = -\log(y!)$, a Poisson regression is obtained. In addition, ϕ is a known dispersion parameter, and ψ is a link function. We write

$$\psi_i = \psi(\mu_i), \quad \mu_i = \mathbb{E}[y_i|X, P].$$

We assume that the expected network-linked response vector $\mu = \mathbb{E}[Y|X, P]$ depends on the column space spanned by X , denoted by $\text{col}(X)$, and a network individual effect vector

$$\omega \in S_K(P) \subset \mathbb{R}^n$$

through a link function, where $S_K(P)$ is the linear subspace spanned by the K leading eigenvectors of P . The assumption that α belongs to $S_K(P)$ is natural and supported by existing evidence that leading eigenvectors of the relational matrix typically capture crucial network information [Özgür et al., 2008, Zeng et al., 2018, Van den Bos et al., 2018, Lee, 2019]. In particular, building on the modeling approach outlined in Le and Li [2022], we assume that μ is contained in the Minkowski sum of $\text{col}(X)$ and $S_K(P)$ through the link function h^{-1} , which is assumed to be *smooth* and *increasing*:

$$h^{-1} \circ \mu = Xv + \omega \in \text{col}(X) + S_K(P) := \{u + v \mid u \in \text{col}(X), v \in S_K(P)\}. \quad (2)$$

Here, by slight abuse of notation, we use $h^{-1} \circ \mu$ to denote the vector of values of h^{-1} evaluated at entries of μ .

A special and important case for h^{-1} is the *natural link function* where

$$h^{-1} = \psi, \quad \text{which implies} \quad \psi_i = x_i^\top v + \omega_i, \quad 1 \leq i \leq n.$$

For example, the logistic regression assumes the natural link function $h^{-1}(\mu) = \log(\frac{\mu}{1-\mu})$ and Poisson regression assumes the natural link function $h^{-1}(\mu) = \log(\mu)$.

Note that $\text{col}(X)$ and $S_K(P)$ may share a non-trivial subspace intersection, which occurs when both X and P depend on certain latent variables such as node cluster information. To ensure identifiability, we decompose $\text{col}(X) + S_K(P)$ based on the subspace intersection

$$\mathcal{R} = \text{col}(X) \cap S_K(P),$$

and parameterize the model as follows.

Definition 2.1 (Network subspace generalized linear model). *Consider a reparametrization of model (1) as*

$$h^{-1} \circ \mu = X\beta^* + \xi^* + \alpha^*, \quad (3)$$

where $\beta^* \in \mathbb{R}^p$ and $\xi^*, \alpha^* \in \mathbb{R}^n$ satisfy

$$\xi^* = X\theta^* \in \mathcal{R}, \quad X\beta^* \perp \mathcal{R}, \quad \alpha^* \in S_K(P), \quad \alpha^* \perp \mathcal{R}. \quad (4)$$

It is straightforward to show that the parameterization in Definition 2.1 is identifiable. That is, if there exist (β, α, θ) and $(\beta', \alpha', \theta')$ satisfying (3) and (4) simultaneously, then $\beta = \beta', \alpha = \alpha'$, and $\theta = \theta'$.

2.3 Model fitting by the subspace-constrained maximum likelihood

We now describe the model fitting procedure for the network subspace generalized linear model. For ease of presentation, let us first outline this procedure assuming we observe $S_K(P)$. At a high level, we want to use the restricted maximum likelihood estimator (MLE) under the subspace constraint under Definition 2.1. Therefore, the estimation is done by solving the following optimization problem:

$$\begin{aligned} & \text{maximize}_{\beta, \xi, \alpha} \quad \mathcal{L}(\beta, \xi, \alpha; Y, X) \\ & \text{subject to} \quad \alpha, \beta, \xi \text{ satisfy (4)} \end{aligned} \quad (5)$$

where $\mathcal{L}(\beta, \xi, \alpha; Y, X)$ is the log-likelihood of the data. To handle the subspace constraint in the optimization, we will introduce a reparameterization of our model for the estimation.

Reparameterization. Using (4), we first rewrite (3) in a more convenient form for estimation purposes. Denote by $\bar{Z} \in \mathbb{R}^{n \times p}$ a matrix whose columns form an orthonormal basis of the covariate subspace $\text{col}(X)$. Similarly, let $\bar{W} \in \mathbb{R}^{n \times K}$ be the matrix whose columns are eigenvectors of P that span the subspace $S_K(P)$. The singular value decomposition of matrix $\bar{Z}^\top \bar{W}$ takes the form

$$\bar{Z}^\top \bar{W} = U \Sigma V^\top.$$

Here, $U \in \mathbb{R}^{p \times p}$ and $V \in \mathbb{R}^{K \times K}$ are orthonormal matrices of singular vectors, while $\Sigma \in \mathbb{R}^{p \times K}$ is the matrix with the following singular values on the main diagonal:

$$\sigma_1 = \sigma_2 = \dots = \sigma_r = 1 > \sigma_{r+1} \geq \dots \geq \sigma_{r+s} > 0 = \sigma_{r+s+1} = \dots = 0. \quad (6)$$

To calculate a basis for the intersection subspace \mathcal{R} , let us denote

$$Z = \sqrt{n} \bar{Z} U, \quad W = \sqrt{n} \bar{W} V. \quad (7)$$

It follows that

$$\mathcal{R} = \text{col}(Z_{1:r}) = \text{col}(W_{1:r}),$$

where $Z_{1:r} \in \mathbb{R}^{n \times r}$ is the submatrix of the first r columns of Z and $W_{1:r}$ is similarly defined. Note that the factor \sqrt{n} ensures that entries of Z , W , and X are generally of comparable magnitudes. We use

$$\mathcal{C} = \text{col}(Z_{(r+1):p}), \quad \mathcal{N} = \text{col}(W_{(r+1):K})$$

to denote the complement subspaces of \mathcal{R} within $\text{col}(X)$ and $S_K(P)$, respectively. With these notations,

$$\text{col}(X) + S_K(P) = \mathcal{R} + \mathcal{C} + \mathcal{N}.$$

Therefore, there exists a vector $\gamma^* \in \mathbb{R}^{p+K-r}$ such that equation (3) is equivalent to

$$h^{-1} \circ \mu = Z_{1:r} \gamma_{1:r}^* + Z_{(r+1):p} \gamma_{(r+1):p}^* + W_{(r+1):K} \gamma_{(p+1):(p+K-r)}^* = \begin{bmatrix} Z & W_{(r+1):K} \end{bmatrix} \gamma^*, \quad (8)$$

where, for any positive integers $s \leq t$, we use $\gamma_{s:t}^* \in \mathbb{R}^{t-s+1}$ to denote the sub-vector of γ^* with entries indexed by integers between s and t . Note that our parameters of interest are ultimately

θ^* , β^* , and α^* , which can be calculated from γ^* as follows:

$$\theta^* = (X^\top X)^{-1} X^\top Z_{1:r} \gamma_{1:r}^*, \quad (9)$$

$$\beta^* = (X^\top X)^{-1} X^\top Z_{(r+1):p} \gamma_{(r+1):p}^*, \quad (10)$$

$$\alpha^* = W_{(r+1):K} \gamma_{(p+1):(p+K-r)}^*. \quad (11)$$

Although Z , W , and γ^* depend on the choice of bases for $\text{col}(X)$ and $S_K(P)$, parameters θ^* , β^* , and α^* are invariant with respect to such choice. With these formulas, the problem of estimating parameters in (4) is equivalent to estimating γ^* , based on an arbitrary basis Z and W corresponding to the true P .

Estimating equation – the ideal case. We now proceed to estimate γ^* . In light of equation (8), let us first denote the i -th row of matrix $(Z \ W_{(r+1):K})$ by g_i^\top , or equivalently,

$$g_i = (Z_{i,1:p} \quad W_{i,(r+1):K})^\top \in \mathbb{R}^{p+K-r}.$$

Viewing g_i as a new covariate vector for the i -th observation turns the model of Definition 2.1 into a typical generalized linear model with parameter γ^* (if we do know g_i 's). Using the first-order stationary condition and setting the gradient of the likelihood function to zero lead to the following estimating equation:

$$S(\gamma) = \frac{1}{n} \sum_{i=1}^n g_i \frac{h'(g_i^\top \gamma)}{v(g_i^\top \gamma)} (y_i - h(g_i^\top \gamma)) = 0, \quad (12)$$

where $h'(\cdot)$ is the derivative of the link function and $v(g_i^\top \gamma)$ is the variance of y_i . Taking the partial derivative of $-S(\gamma)$, we obtain the oracle information matrix

$$F(\gamma) = \frac{1}{n} \sum_{i=1}^n \frac{(h'(g_i^\top \gamma))^2}{v(g_i^\top \gamma)} g_i g_i^\top. \quad (13)$$

Later on, this matrix will be used to approximate the asymptotic variance in (16). It is unique up to a rotation due to the choice of basis for $\text{col}(X)$ and $S_K(P)$.

Sample version estimators. In practice, instead of observing the relational matrix P directly, we only have access to a noisy version \hat{P} of P . We replace P with \hat{P} everywhere in the above procedure. In particular, let $\tilde{W} \in \mathbb{R}^{n \times K}$ be the matrix whose columns are eigenvectors of \hat{P} that span the subspace $S_K(\hat{P})$. The singular value decomposition of $\tilde{Z}^\top \tilde{W}$ takes the form

$$\tilde{Z}^\top \tilde{W} = \tilde{U} \tilde{\Sigma} \tilde{V}^\top.$$

Similarly, denote

$$\tilde{Z} = \sqrt{n} \tilde{Z} \tilde{U}, \quad \tilde{W} = \sqrt{n} \tilde{W} \tilde{V}. \quad (14)$$

We always assume that r , the dimension of \mathcal{R} , is known, as a consistent estimate of r is already provided by Le and Li [2022]. With this assumption, we estimate \mathcal{R} , \mathcal{C} , and \mathcal{N} by

$$\hat{\mathcal{R}} = \text{col}(\tilde{Z}_{1:r}), \quad \hat{\mathcal{C}} = \text{col}(\tilde{Z}_{(r+1):p}), \quad \hat{\mathcal{N}} = \text{col}(\tilde{W}_{(r+1):K}). \quad (15)$$

The sample version of the estimating equation takes the form

$$\tilde{S}(\gamma) = \frac{1}{n} \sum_{i=1}^n \tilde{g}_i \frac{h'(\tilde{g}_i^\top \gamma)}{v(\tilde{g}_i^\top \gamma)} \left(y_i - h(\tilde{g}_i^\top \gamma) \right) = 0, \quad (16)$$

where \tilde{g}_i denote the i -th row vector of matrix $[\tilde{Z} \quad \tilde{W}_{(r+1):K}]$. We solve this equation using the iteratively reweighted least squares method [Green, 1984]. Finally, the sample information matrix is given by

$$\tilde{F}(\gamma) = \frac{1}{n} \sum_{i=1}^n \frac{(h'(\tilde{g}_i^\top \gamma))^2}{v(\tilde{g}_i^\top \gamma)} \tilde{g}_i \tilde{g}_i^\top. \quad (17)$$

A summary of this procedure is given in Algorithm 3. It is worth mentioning that our algorithm requires access to K . Since the problem of estimating K has been extensively studied [Li et al., 2020, Le and Levina, 2022, Han et al., 2023], we will assume throughout this paper that K is known.

Algorithm 1: Subspace Maximum Likelihood Estimation Algorithm

Input: Design Matrix $X \in \mathbb{R}^{n \times p}$, response vector $Y \in \mathbb{R}^n$, estimated relational matrix $\hat{P} \in \mathbb{R}^{n \times n}$ and dimension of the intersection subspace r .

Output: Estimators $\hat{\theta}$, $\hat{\beta}$, and $\hat{\alpha}$.

- 1 Calculate the orthonormal basis of $\text{col}(X)$ and form matrix $Z \in \mathbb{R}^{n \times p}$ in (7); calculate K eigenvectors of \hat{P} and form $\check{W} \in \mathbb{R}^{n \times K}$.
 - 2 Calculate the singular value decomposition $Z^T \check{W} = \tilde{U} \tilde{\Sigma} \tilde{V}^T$, and form $\tilde{Z} = \sqrt{n} Z \tilde{U}$, $\tilde{W} = \sqrt{n} \check{W} \tilde{V}$.
 - 3 Find the root $\hat{\gamma}$ of the generalized estimating equation $\tilde{S}(\gamma) = 0$ using the iteratively reweighted least squares method, and obtain $\hat{\theta}, \hat{\beta}, \hat{\alpha}$ by replacing γ with $\hat{\gamma}$ in (9), (10), and (11), respectively.
-

3 Statistical Inference Properties

This section provides theoretical results for the estimation consistency and statistical inference of the proposed method. To this end, we need the following regularity conditions.

Assumption 1 (Scaling). $\|X_j\| = \sqrt{n}$ for all columns of X . In addition, there exists a constant C such that $\|X\beta^*\|$, $\|X\theta^*\|$ and $\|\alpha^*\|$ are bounded by $C\sqrt{n}$.

Assumption 2 (Well-conditioned covariates). There exists a constant $C > 0$ such that $G = (X^\top X/n)^{-1}$ satisfies

$$1/C \leq \lambda_{\min}(G) \leq \lambda_{\max}(G) \leq C.$$

Assumption 3 (Boundedness of X and W). There exists a constant $C > 0$ such that $\|g_i\| \leq C$ for all $1 \leq i \leq n$.

Assumption 4 (Well-conditioned Information Matrix). There exists constants $\delta, C > 0$ such that when $\|\gamma - \gamma^*\| < \delta$ the oracle information matrix defined in (13) satisfies that

$$1/C \leq \lambda_{\min}(F(\gamma)) \leq \lambda_{\max}(F(\gamma)) \leq C.$$

Assumption 5 (Small Projection Perturbation). *The approximate relational matrix \hat{P} satisfies*

$$\bar{\tau}_n := n^{-3/2} \frac{\|(\tilde{W}\tilde{W}^T - WW^T)Z\|}{\min \left\{ (1 - \sigma_{r+1})^3, \sigma_{r+s}^3 \right\}},$$

for any n , where σ_{r+1} and σ_{r+s} are the singular values in (6), and

$$\bar{\tau}_n = o(n^{-1/2}).$$

Assumption 5 is our essential requirement for the network perturbation level that is tolerable. This assumption is also used in Le and Li [2022], which is shown to be reasonable for network perturbations in many cases. In Section 4, we will show that this is valid to handle many real-world applications.

Assumption 6 (Moment Constraint for Responses). *There exists constants $c > 0$, $M_0 > 0$ and $\xi > 2$ such that*

$$\min_{1 \leq i \leq n} \text{Var}(y_i) > c, \quad \mathbb{E}|y_i - \mathbb{E}[y_i]|^\xi < M_0.$$

Assumption 6 provides a sufficient condition for the Lindeberge-Feller Central Limit Theorem to hold. A similar constraint has been adopted in Yin et al. [2006], Gao et al. [2012].

Theorem 1 (Existence and Consistency). *Consider the estimating equation (16) and assume that Assumptions 1–6 hold. For each n , there exists $\hat{\gamma}$ such that as $n \rightarrow \infty$,*

$$\mathbb{P}(\tilde{S}(\hat{\gamma}) = 0) \rightarrow 1. \quad (18)$$

Moreover, the corresponding estimates $\hat{\theta}, \hat{\beta}$, and $\hat{\alpha}$, obtained by replacing γ^* with $\hat{\gamma}$ in (9), (10), and (11), respectively, satisfy

$$\|\hat{\theta} - \theta^*\| = o_p(1), \quad \|\hat{\beta} - \beta^*\| = o_p(1), \quad \|\hat{\alpha} - \alpha^*\| = o_p(n^{1/2}). \quad (19)$$

Theorem 1 shows that for each n , there exists a solution to the estimating equation (16) with high probability. In addition, the sequences of corresponding estimates for the true parameters in (3) are consistent. It is worth noting that similar to Yin et al. [2006], Theorem 1 itself does not guarantee the uniqueness of the solution $\hat{\gamma}$. This is because the log-likelihood function is generally not concave for special link functions. However, Corollary 2 below shows that restricting the model space to the class with natural links functions, or more generally, link functions ensuring concavity, leads to the uniqueness.

Corollary 2 (Uniqueness). *Assume that Assumptions 1 to 6 hold and the link function is natural. That is, $h^{-1} = \psi$. Then the estimates in Theorem 1 are unique for sufficiently large n .*

Our next result concerns the asymptotic distributions of the proposed estimates for θ^* , β^* , and α^* . Since these parameters depend on γ^* through equations (9), (10), and (11), we need the covariance matrices of $\hat{\gamma}_{1:r}$, $\hat{\gamma}_{(r+1):p}$, and $\hat{\gamma}_{(p+1):(p+K-r)}$. These matrices can be estimated by the diagonal blocks of the inverse of the sample information matrix in (17), which we denote by $\tilde{F}_1^{-1}(\hat{\gamma})$,

$\tilde{F}_2^{-1}(\hat{\gamma})$, and $\tilde{F}_3^{-1}(\hat{\gamma})$, respectively. Thus,

$$\tilde{F}^{-1}(\hat{\gamma}) = \begin{pmatrix} \tilde{F}_1^{-1}(\hat{\gamma}) & * & * \\ * & \tilde{F}_2^{-1}(\hat{\gamma}) & * \\ * & * & \tilde{F}_3^{-1}(\hat{\gamma}) \end{pmatrix},$$

where $\tilde{F}_1^{-1}(\hat{\gamma}) \in \mathbb{R}^{r \times r}$, $\tilde{F}_2^{-1}(\hat{\gamma}) \in \mathbb{R}^{(p-r) \times (p-r)}$, and $\tilde{F}_3^{-1}(\hat{\gamma}) \in \mathbb{R}^{(K-r) \times (K-r)}$. In addition, we use $\kappa(\hat{\gamma}) \in \mathbb{R}^{n \times n}$ to denote the diagonal matrix with entries $(h'(\tilde{g}_i^\top \hat{\gamma}))^2 / v(\tilde{g}_i^\top \hat{\gamma})$, $1 \leq i \leq n$, on the diagonal:

$$\kappa(\hat{\gamma}) = \text{diag} \left(\frac{(h'(\tilde{g}_i^\top \hat{\gamma}))^2}{v(\tilde{g}_i^\top \hat{\gamma})} \right).$$

We are now ready to state the asymptotic distributions of the proposed estimates.

Theorem 3 (Asymptotic Distributions). *Assume that Assumptions 1 to 6 hold. For each n , let $\hat{\theta}$, $\hat{\beta}$, and $\hat{\alpha}$, be the estimates based on $\hat{\gamma}$ satisfying Theorem 1. We have the following results.*

(a) *As n tends to infinity,*

$$n \left(\hat{\alpha} - \frac{1}{n} \tilde{W}_{(r+1):K} \tilde{W}_{(r+1):K}^\top \alpha^* \right)^\top \tilde{O} \left(\hat{\alpha} - \frac{1}{n} \tilde{W}_{(r+1):K} \tilde{W}_{(r+1):K}^\top \alpha^* \right) \rightarrow \chi_{K-r}^2, \quad (20)$$

in distribution, where χ_{K-r}^2 denotes the χ^2 distribution with $K-r$ degrees of freedom, and $\tilde{O} = n^{-1} \left(\kappa(\hat{\gamma}) - \kappa(\hat{\gamma}) \tilde{Z} \left(\tilde{Z}^\top \kappa(\hat{\gamma}) \tilde{Z} \right)^{-1} \tilde{Z}^\top \kappa(\hat{\gamma}) \right)$.

(b) *For any fixed unit vector $u \in \mathbb{R}^p$, assume that*

$$n^{-1} \|Z_{(r+1):p}^\top XGu\| \geq c \quad (21)$$

for some constant $c > 0$ and sufficiently large n . Then,

$$\frac{\sqrt{n}(u^\top \hat{\beta} - u^\top \beta^*)}{n^{-1} \left(u^\top GX^\top \tilde{Z}_{(r+1):p} \tilde{F}_2^{-1}(\hat{\gamma}) \tilde{Z}_{(r+1):p}^\top XGu \right)^{1/2}} \rightarrow \mathcal{N}(0, 1), \quad (22)$$

where $\mathcal{N}(0, 1)$ denotes the standard normal distribution.

(c) *Similarly, for any fixed unit vector $u \in \mathbb{R}^p$, assume that*

$$n^{-1} \|Z_{1:r}^\top XGu\| \geq c \quad (23)$$

for some constant $c > 0$ and sufficiently large n . Then,

$$\frac{\sqrt{n}(u^\top \hat{\theta} - u^\top \theta^*)}{n^{-1} \left(u^\top GX^\top \tilde{Z}_{1:r} \tilde{F}_1^{-1}(\hat{\gamma}) \tilde{Z}_{1:r}^\top XGu \right)^{1/2}} \rightarrow \mathcal{N}(0, 1). \quad (24)$$

To understand condition (21), note that according to (10), $u^\top \beta^*$ lies in the linear space spanned by coordinates of $Z_{(r+1):p}^\top XGu$. Condition (21) essentially requires that this space is not vanishing or degenerate. Otherwise, the inference of $u^\top \beta^*$ would not be meaningful. Condition (23) has a

similar interpretation. These conditions are also needed in Le and Li [2022]. Note also that in Theorem 3, $n^{-1}\|\tilde{Z}_{(r+1):p}^T XGu\|$, $n^{-1}\|\tilde{Z}_{1:r}^T XGu\|$, and \tilde{O} are invariant to the choices of bases for $S_K(\hat{P})$ and $\text{col}(X)$.

Corollary 2 and Theorem 3 provide the asymptotic distributions for $\hat{\alpha}$, $\hat{\beta}$, and $\hat{\theta}$ that can be used for inference purposes. In particular, (20), (24), and (22) allow us to test the presence of pure network effect (against $\alpha^* = 0$), pure covariate effect (against $\theta^* = 0$), and the shared information between the two (against $\beta^* = 0$), respectively. For example, when testing against $H_0 : \alpha^* = 0$, Theorem 3 indicates that we can use $n\hat{\alpha}^T \tilde{O} \hat{\alpha}$ as the statistic for a χ^2 test.

4 Simulation Studies

We now introduce a sequence of simulation experiments to evaluate the proposed method. In particular, we want to demonstrate the effectiveness of the proposed method in model estimation and statistical inference under two types of perturbation mechanisms for network structures: random network model perturbations and embedding perturbations from deep learning embedding algorithms. We will evaluate two specific models in our model class: the subspace logistic regression and the subspace Poisson regression.

4.1 Perturbations from random network models

We first study the performance of the proposed methods when the observed networks are subject to the perturbations introduced by random network models. In particular, the true relational matrix P in our model is assumed to be a probability matrix taking values in $[0, 1]$. Our true model is defined based on $S_K(P)$. The observed network is generated from P following the so-called “inhomogeneous Erdős-Rényi” framework: for each $i < j, i, j \in [n]$, generate the adjacency matrix $A_{ij} \sim \text{Bernoulli}(P_{ij})$. Different matrices P tend to generate networks with different structures and the perturbation comes from the randomness of this generating process.

Random network models. Regarding the network generative mechanisms, we use two low-rank models and a full-rank model. The stochastic block model (SBM) of Holland et al. [1983] with three communities, and the out-in-ratio between blocks is set to be 0.3. The degree-corrected block model (DCBM) of Karrer and Newman [2011], where the community connection matrix is the same as the SBM with additional degree parameters varying from 0.2 to 1 (before rescaling). These two models are generated by the R package *randnet* [Li et al., 2023]. The full-rank model is the one from Zhang et al. [2017], in which P is constructed from the graphon function $g(\mu, \nu) = c/\{1 + \exp[15(0.8|\mu - \nu|)^{4/5} - 0.1]\}$. This graphon model gives a banded matrix along the diagonal. So we call it the “diagonal graphon” model. In all experiments, we vary the sample size n from 500 to 4000, and the expected average degree is set to be $\varphi_n = 2 \log n, \sqrt{n}, n^{2/3}, n/6$ to demonstrate the effect of varying network density.

Subspace and covariates. Following Le and Li [2022], we construct $X \in \mathbb{R}^{n \times p}$ using the eigenvectors w_1, \dots, w_n from P as follows: Set $X_1/\sqrt{n} = w_1$; Set $X_2/\sqrt{n} = w_2/5 + 2\sqrt{6}w_4/5$. This configuration yields a design with $r = 1, s = 3$. We set $\beta = (0, 0.5)^\top$ and $\theta = (0.5, 0)^\top$ in all settings. Similarly, γ^* can be any vector with the first coordinate being zero, where we set $\gamma^* = (0, 0.5, 0.5)^\top$. In the model fitting process, we always use the observed adjacency matrix A to approximate the true eigenspace.

Evaluation criterion. For model estimation accuracy, we measure the performance by the mean squared error (MSE) on β_2 , defined as $|\hat{\beta}_2 - \beta_2|^2$, the mean square prediction error (MSPE) defined

as $\|\hat{Y} - \mathbb{E}Y\|^2/n$. For inference, we evaluate the coverage probability of the 95% confidence interval for β_2 ¹

Benchmark methods. A standard logistic regression model without the network component was also included for comparison. In addition, we include the RNC method from Li et al. [2019]. The model fitting parameter is chosen by 10-fold cross-validation.

Calculation procedure. In order to assess the model’s performance with the randomness from both the response Y and neighborhood matrix A , we generate 100 unique neighborhood matrices A based on one relational matrix P for each simulation scenario. For each given A , 1000 replicates of Y ’s are generated, and the performance metrics, the coverage probability, and MSE are calculated based on the Monte Carlo approximation from these 1000 instantiations. At the outer loop, we repeatedly generate A 100 times, and the median value of the resulting coverage probabilities and MSEs are reported.

Table 1: Median MSE and coverage probability for subspace logistic regression under random network perturbations.

n	avg.degree	SBM		DCBM		Diag	
		MSE	Coverage	MSE	Coverage	MSE	Coverage
500	$2 \log n$	1.16	94.6%	1.18	95.4%	1.31	92.4%
	\sqrt{n}	1.15	94.8%	1.19	94.8%	1.18	93.8%
	$n^{2/3}$	1.13	95.2%	1.22	95.3%	1.13	94.4%
1000	$2 \log n$	0.56	94.7%	0.56	95.1%	0.64	93.5%
	\sqrt{n}	0.57	94.9%	0.57	95.0%	0.63	93.9%
	$n^{2/3}$	0.58	95.0%	0.57	95.1%	0.60	94.7%
2000	$2 \log n$	0.35	93.1%	0.29	95.1%	0.28	93.7%
	\sqrt{n}	0.31	94.7%	0.28	95.0%	0.27	94.4%
	$n^{2/3}$	0.30	95.1%	0.28	95.1%	0.26	94.9%
4000	$2 \log n$	0.16	92.7%	0.15	94.2%	0.15	93.5%
	\sqrt{n}	0.14	94.9%	0.14	95.0%	0.14	94.6%
	$n^{2/3}$	0.14	95.0%	0.14	95.1%	0.14	94.8%

Table 1 shows how our method performs under the network subspace logistic regression model. Overall, the performance improves with the same size n and the expected average degree of the network model. The denser networks make the problem easier because the concentration of the adjacency matrix to the true P is better. The study by Le and Li [2022] suggests that the small perturbation projection assumption holds true under random network perturbation for networks with an average degree higher than \sqrt{n} . Table 1 confirms this observation.

Table 2 presents the MSE comparison between our model and the two benchmarks. The standard logistic regression has the worst performance as it lacks network information. The RNC method captures general network information with its cohesion penalty, and its effectiveness is not very sensitive to network sparsity. Especially under the simplest SBM, it is empirically known that the penalty can accurately capture community information, as demonstrated by Li et al. [2019]. Therefore, RNC can be accurate under the SBM, with advantages in sparse settings. However, when network degrees are heterogeneous (under the DCBM), RNC loses its effectiveness under the subspace model. Our method remains effective in all cases.

¹The theoretical findings in Theorem 3 suggests that a valid inference cannot be drawn for $\hat{\beta}_1$ for the overlapping effect, similar to Le and Li [2022].

Table 2: Median MSPE ($\times 10^2$) for subspace logistic regression and benchmarks under traditional random network perturbations.

n	Network	avg.degree	Our Model	Logistic Reg	RNC
500	SBM	$2 \log n$	1.11	1.34	1.89
		\sqrt{n}	0.64	1.34	1.88
		$n^{2/3}$	0.31	1.34	1.80
	DCBM	$2 \log n$	1.05	2.48	2.46
		\sqrt{n}	0.60	2.48	2.51
		$n^{2/3}$	0.28	2.48	2.50
	Diag	$2 \log n$	0.38	0.67	1.19
		\sqrt{n}	0.26	0.67	1.11
		$n^{2/3}$	0.18	0.67	1.08
1000	SBM	$2 \log n$	0.96	2.01	0.49
		\sqrt{n}	0.43	2.01	0.51
		$n^{2/3}$	0.18	2.01	0.49
	DCBM	$2 \log n$	0.76	1.99	1.98
		\sqrt{n}	0.40	1.99	1.89
		$n^{2/3}$	0.16	1.99	1.93
	Diag	$2 \log n$	0.32	2.13	1.11
		\sqrt{n}	0.17	2.13	1.28
		$n^{2/3}$	0.10	2.13	1.06

Under the Poisson model, we use the same configuration except for replacing the logistic distribution with the Poisson distribution. The same results are presented in Table 3 and Table 4. In Table 3, the phase transition phenomenon at the expected average degree of \sqrt{n} is clearer than in Table 1. When the average degree surpasses the order of \sqrt{n} , the asymptotic validity holds. Under the diagonal graphon model, the perturbation has a stronger impact, but the inference remains approximately correct with the current sample size for sufficiently dense networks. The overall message remains the same as in the logistic regression setting.

In conclusion, the simulation results indicate that the estimator from our model is asymptotically unbiased and normally distributed when the average degree is $n^{2/3}$ or higher. However, the asymptotic behavior of estimation on sparser networks is influenced by the choice of link function and data scale.

4.2 Network perturbations by from deep-learning-based embedding methods

We now consider another application scenario in which the proposed model can be used. Suppose we want to use embedding methods from deep-learning communities to extract the network information. Multiple recent works [Pozek et al., 2019, Pranathi and Prathibhamol, 2021, Liu and Huang, 2024] take this strategy to incorporate network information, with the belief that these methods can capture high-order network relations more effectively by their highly nonlinear operations.

Our subspace generalized linear model, with its flexibility in specifying a proper subspace $S_K(P)$, can seamlessly leverage this embedding information. Specifically, we can assume the Euclidean similarities of the embedded vectors as the perturbed relational information \hat{P} , with the true relational matrix being an unobserved similarity matrix that can be different from the random embedded similarities. In these cases, even if the network is usually treated as fixed, the embedding algorithms are typically random by nature. This randomness in embeddings raises concerns about

Table 3: Median MSE and coverage probability for subspace Poisson regression under random network perturbations.

n	avg.degree	SBM		DCBM		Diag	
		MSE	Coverage	MSE	Coverage	MSE	Coverage
500	$2 \log n$	0.35	75.8%	0.21	75.2%	0.53	72.4%
	\sqrt{n}	0.16	86.2%	0.11	90.4%	0.38	84.9%
	$n^{2/3}$	0.10	93.5%	0.09	93.8%	0.23	93.4%
1000	$2 \log n$	0.08	87.2%	0.27	29.9%	0.27	57.7%
	\sqrt{n}	0.06	92.9%	0.07	82.4%	0.11	88.8%
	$n^{2/3}$	0.06	94.2%	0.04	93.5%	0.08	93.8%
2000	$2 \log n$	0.06	73.4%	0.14	29.1%	0.09	77.0%
	\sqrt{n}	0.03	92.3%	0.03	86.4%	0.05	91.7%
	$n^{2/3}$	0.03	94.8%	0.02	94.0%	0.04	93.7%
4000	$2 \log n$	0.04	71.4%	0.04	89.8	0.61	0%
	\sqrt{n}	0.01	93.4%	0.01	94.3%	0.06	58.3%
	$n^{2/3}$	0.01	94.5%	0.01	94.6%	0.02	93.0%

the validity of modeling and inference if one uses a specific embedding in the model. In this section, we use simulation experiments to evaluate the validity of our model’s inference under such permutations of embeddings. The study of statistical properties of the embedding methods is rare in literature. The only one we know is from [Zhang and Tang \[2023\]](#) on community detection. To our knowledge, the current experiment is the first empirical study in the literature to investigate the deep-learning-based network embedding methods’ impacts on downstream statistical inference tasks.

We consider three popular network embedding methods, DeepWalk [[Perozzi et al., 2014](#)], Node2Vec [[Grover and Leskovec, 2016](#)], and Diff2Vec [[Rozemberczki and Sarkar, 2018](#)] to demonstrate these scenarios. DeepWalk was one of the earliest graph embedding methods from the deep learning community, and Node2Vec is a generalization of DeepWalk. Diff2Vec uses the more recent diffusion framework to define the embeddings. The implementations of DeepWalk and Node2Vec are available in the Python package *node2vec* [[Grover and Leskovec, 2016](#)], and Diff2Vec is implemented in the Python package *karateclub* [[Rozemberczki et al., 2020](#)]. In our simulation, we always use the recommended configurations of these methods. For DeepWalk and Node2Vec, each embedding is based on 10 walks per node of length 80. For Node2Vec, the return probability is set to 0.5. For Diff2Vec, we use 20 trees per node of size 80. The network embedding dimension is always set to 3.

Design of relational matrix. We first generate a network A from one of the three models in Section 4.1, and fix the network A . Given A , all three embedding methods are random and result in different embeddings each time. Therefore, for each embedding method, suppose \mathcal{F} is the embedding of A and, intuitively, we can use $\mathcal{F}\mathcal{F}^\top$ as the available similarity matrix we can use from data. The perturbation of network information comes from the randomness of \mathcal{F} . Specifically, in this context, we set the true relational matrix as the oracle central similarity $P = \mathbb{E}[\mathcal{F}\mathcal{F}^\top]$, and $\hat{P} = \mathcal{F}\mathcal{F}^\top$. The design matrix X and other quantities are generated in the same manner as in Section 4.1 based on the current P .

Table 5 and Table 6 illustrate all the performance metrics under the perturbation of different embedding algorithms on the three network types with varying average degrees when $n = 2000$. Note that the previous benchmark method, RNC, is not applicable in this new setting and was

Table 4: Median MSPE for subspace Poisson regression and benchmarks under traditional random network perturbations.

n	Network	avg.degree	Our Model	Poisson Reg	RNC
500	SBM	$2 \log n$	2.30	2.81	1.49
		\sqrt{n}	1.41	2.81	1.56
		$n^{2/3}$	0.53	2.81	1.67
	DCBM	$2 \log n$	1.09	2.58	1.41
		\sqrt{n}	0.72	2.58	1.55
		$n^{2/3}$	0.32	2.58	1.33
	Diag	$2 \log n$	0.44	1.11	0.92
		\sqrt{n}	0.25	1.11	0.90
		$n^{2/3}$	0.07	1.11	0.93
1000	SBM	$2 \log n$	1.66	4.20	1.34
		\sqrt{n}	0.82	4.20	1.35
		$n^{2/3}$	0.27	4.20	1.23
	DCBM	$2 \log n$	0.96	5.58	1.75
		\sqrt{n}	0.58	5.58	1.73
		$n^{2/3}$	0.21	5.58	1.64
	Diag	$2 \log n$	0.22	0.74	1.30
		\sqrt{n}	0.09	0.74	1.20
		$n^{2/3}$	0.03	0.74	1.28

removed from the comparison. This also demonstrates the flexibility of our subspace-based model.

For each of the three embedding mechanisms, the estimation accuracy and inference correctness (measured by the coverage probability) exhibit mild improvements with the increase of network density. Among the three mechanisms, Diff2Vec is more sensitive to network density. For example, on networks with an average degree of $2 \log n$, the coverage probability misses the target level by about 5%. DeepWalk and Node2Vec are more robust. Overall, the impact of network density is weaker on all embedding mechanisms compared to the random network perturbation mechanisms. The most important observation from these experimental results is that our model estimation remains accurate, and the statistical inference is still approximately correct unless the network is very sparse. This result demonstrates the applicability of our inference framework in broader scenarios in modern machine learning.

5 Social and Educational Effect Study of School Conflicts

With the proposed model, we will analyze data from the school conflict study introduced in Section 1.1. Following the original strategy of Paluck et al. [2016], we use the allocation of orange wristbands to examine the impact of anti-conflict interventions on behaviors that promote a positive school climate, rewarding actions that are friendly or conflict-mitigating. If a student receives an orange wristband, the response variable Y is set to 1; otherwise, it is 0. We employ a logistic model to analyze this response.

To identify features strongly associated with the allocation of orange wristbands, we use individual attributes from the supplementary materials of Paluck et al. [2016] as potential predictors. These include Treatment (participation in weekly training: Yes/No), Gender (Male/Female), Race (White/Hispanic/Black/Asian/Others), Grade, “Friends-like-house” (friends say I have a nice

Table 5: Median MSE, coverage probability for subspace logistic regression with different types of network of size 2000 under network embedding perturbations.

Method	Network	avg.degree	MSE	Coverage	MSPE	
					Our Model	Logistic Reg
DeepWalk	SBM	$2 \log n$	0.30	94.4%	0.08	1.30
		\sqrt{n}	0.29	94.8%	0.07	2.18
		$n^{2/3}$	0.29	94.7%	0.08	1.90
	DCBM	$2 \log n$	0.48	94.5%	0.09	1.90
		\sqrt{n}	0.32	94.8%	0.08	0.71
		$n^{2/3}$	0.30	94.8%	0.08	1.68
	Diag	$2 \log n$	0.31	95.0%	0.04	1.17
		\sqrt{n}	0.29	95.0%	0.05	1.17
		$n^{2/3}$	0.29	95.0%	0.05	1.24
Node2Vec	SBM	$2 \log n$	0.30	94.3%	0.09	1.80
		\sqrt{n}	0.28	94.8%	0.08	2.08
		$n^{2/3}$	0.29	94.9%	0.08	2.08
	DCBM	$2 \log n$	0.37	94.7%	0.08	1.09
		\sqrt{n}	0.32	94.8%	0.08	1.17
		$n^{2/3}$	0.30	94.8%	0.08	1.79
	Diag	$2 \log n$	0.31	94.9%	0.05	0.88
		\sqrt{n}	0.29	95.0%	0.05	1.21
		$n^{2/3}$	0.29	95.1%	0.05	1.18
Diff2Vec	SBM	$2 \log n$	0.32	93.5%	0.10	1.07
		\sqrt{n}	0.30	94.8%	0.07	1.21
		$n^{2/3}$	0.30	94.6%	0.07	1.08
	DCBM	$2 \log n$	0.30	94.2%	0.10	1.15
		\sqrt{n}	0.32	94.4%	0.08	1.10
		$n^{2/3}$	0.30	94.6%	0.07	0.99
	Diag	$2 \log n$	0.30	93.8%	0.12	1.22
		\sqrt{n}	0.33	94.7%	0.09	1.19
		$n^{2/3}$	0.32	94.8%	0.08	1.14

house: Yes/No), and Home-language (speaks another language at home: Yes/No). Additionally, we incorporate GPA (grade point average on a 4.0 scale) and a binary covariate, Influencer (nominated by the teacher as influential). A school-specific effect parameter is included for each school to account for school-level differences. We use the largest connected components from each school, removing students with incomplete information. After data processing, we have data on 8685 students from 25 schools, with 1391 students receiving an orange wristband. Based on our evaluation, embedding methods such as Node2Vec do not improve predictive performance (see Section A.3) for the current dataset. Therefore, we will directly use the observed networks for better interpretability and to align with the original analysis of Paluck et al. [2016].

5.1 Model fitting and interpretations

We use the average of two friendship adjacency matrices from two survey waves (at the start and end of the school year) as our weighted adjacency matrix to measure the relations between students. It turns out that using either matrix alone yields the same analysis, thanks to the robustness of

Table 6: Median MSE, coverage probability for subspace Poisson regression with different types of network of size 2000 under network embedding perturbations.

Method	Network	avg.degree	MSE	Coverage	MSPE	
					Our Method	Poisson Reg
DeepWalk	SBM	$2 \log n$	0.06	92.9%	1.99	28.6
		\sqrt{n}	0.06	94.0%	1.58	45.1
		$n^{2/3}$	0.06	93.8%	1.27	22.4
	DCBM	$2 \log n$	0.07	91.8%	2.70	41.1
		\sqrt{n}	0.04	93.7%	2.21	19.4
		$n^{2/3}$	0.06	93.8%	1.59	21.1
	Diag	$2 \log n$	0.07	94.9%	0.91	12.2
		\sqrt{n}	0.05	94.8%	0.65	23.5
		$n^{2/3}$	0.05	94.7%	0.63	25.4
Node2Vec	SBM	$2 \log n$	0.08	93.2%	1.93	40.8
		\sqrt{n}	0.06	93.7%	1.54	35.1
		$n^{2/3}$	0.07	94.0%	1.23	24.7
	DCBM	$2 \log n$	0.06	91.9%	2.77	60.7
		\sqrt{n}	0.05	94.0%	2.23	22.1
		$n^{2/3}$	0.05	93.7%	2.40	18.0
	Diag	$2 \log n$	0.06	94.7%	0.62	19.2
		\sqrt{n}	0.06	94.7%	0.61	21.6
		$n^{2/3}$	0.05	94.5%	0.69	21.3
Diff2Vec	SBM	$2 \log n$	0.09	87.7%	2.58	22.1
		\sqrt{n}	0.07	94.0%	1.19	34.7
		$n^{2/3}$	0.07	93.9%	1.42	13.4
	DCBM	$2 \log n$	0.07	93.2%	2.41	26.4
		\sqrt{n}	0.07	93.7%	1.85	20.7
		$n^{2/3}$	0.06	93.0%	1.59	10.0
	Diag	$2 \log n$	0.12	90.5%	1.31	17.2
		\sqrt{n}	0.07	93.9%	0.86	15.0
		$n^{2/3}$	0.08	94.4%	0.67	15.1

our framework to network perturbations (see Section A.2). This is a crucial advantage of our framework.

Under our model, using the full dataset, the χ^2 test for network effects gives a very small p-value ($< 10^{-8}$), indicating a significant contribution of the network information. The estimated $\hat{\alpha}_i$'s are shown in Figure 2. The corresponding estimated coefficients of covariates are included in Section A in Appendix. The network effects show considerable variation in magnitude across different schools, with strong social impacts observed in a few schools, while in most others, the social network impact is minor. Consequently, we focus our analysis on the schools with strong network effects for deeper insights.

We define a school-specific network-effect-strength $t_j := \sum_{i \in O_j} |\hat{\alpha}_i| / \sum_{i \in O_j} |x_i^\top \hat{\beta}|$, where O_j is the index of students in the j th school. We select the five schools with the largest t_j values (Schools 1, 22, 27, 31, and 48) for further analysis. We then apply our SP logistic model, standard logistic regression, and the RNC logistic regression to the data. For our model and the standard logistic

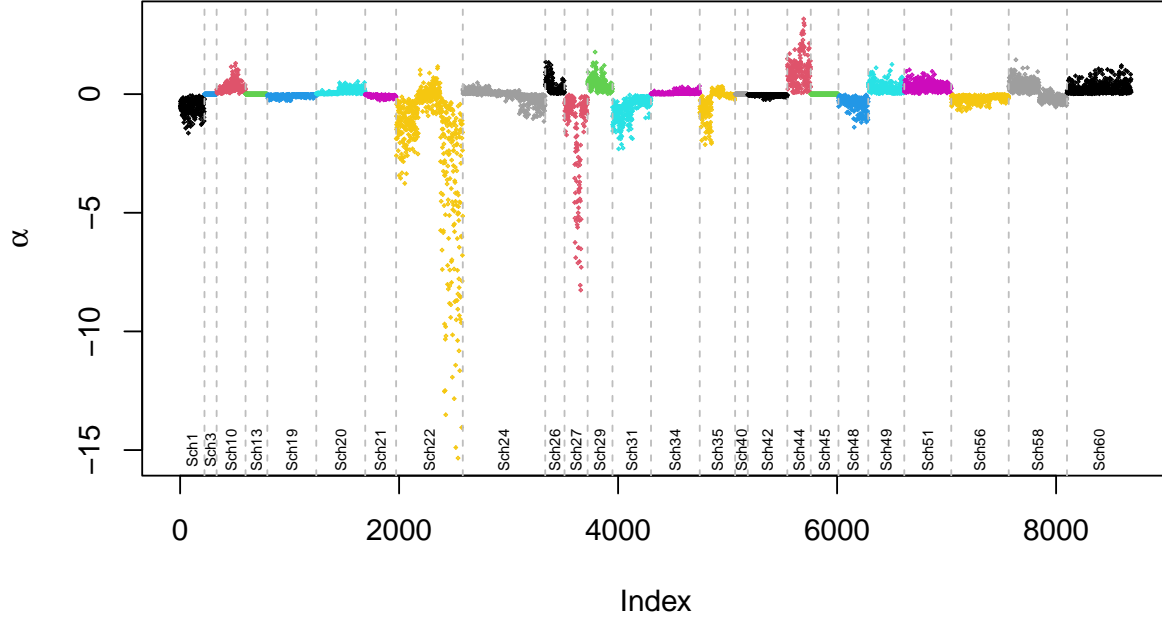


Figure 2: Fitted $\hat{\alpha}$ from our model

regression, important predictors are selected using backward elimination, whereby variables with the largest p-values exceeding 0.05 after Bonferroni correction are removed sequentially until no further elimination is possible. As the RNC model lacks an inference framework, we retain all variables in that model. The results of the three fitted models and their corresponding p-values are summarized in Table 7.² School-specific effects are not included in the table.

Again, our χ^2 test gives a very small p-value, providing strong evidence of social effects. The coefficient for Treatment is estimated similarly by all three models. This is expected since, in the study, whether a student is enrolled in the training is randomly determined by the experiment design, making this variable uncorrelated with any other effects. However, unlike the RNC, our method and the standard logistic regression can use their p-values to show that the treatment effect is indeed significant. This finding aligns with the analysis of Paluck et al. [2016], which used a more sophisticated causal inference framework to study the data with the design information.

Since the RNC does not provide inference and variable selection, we focus on comparing our method with standard logistic regression. The two models yield very different inferences for the effects of Gender, Grade, and Race. Notably, Gender is the only predictor besides Treatment that remains in the final selection based on our model. The standard logistic regression estimates a 25% stronger gender effect and finds statistically significant negative effects for Grade and Race. The main difference between our model and standard logistic regression is the inclusion of network effects, suggesting that the differential predictors may be cohesive according to network structures. This phenomenon is intuitively reasonable. For example, students are more likely to be friends

²Note that the p-values do not account for the selection of the five schools based on data and the backward elimination of variables. These results are used primarily for qualitative interpretations. In Section 5.2, we validate the models more rigorously through prediction performance, with the randomness of the selection procedure accounted for.

Table 7: Model fitting and inference results on five schools with strongest effect schools.

	Our Model		Logistic Reg		RNC	
	coef.	p-value	coef.	p-value	coef.	p-value
Treatment	0.644	$< 10^{-3}$	0.629	$< 10^{-3}$	0.698	
Gender:Male	-0.450	$< 10^{-3}$	-0.568	$< 10^{-3}$	-0.486	
Grade			-0.180	0.002	-0.317	
Friends like House					-0.055	
Home Language					0.163	
GPA					-0.183	
Influencer					0.544	
Race:White			-0.701	$< 10^{-3}$	-0.431	
Race:Black					-0.142	
Race:Hispanic			-0.724	$< 10^{-3}$	-0.491	
Race:Asian					0.222	
Network Effect	—	8.5×10^{-3}	—	—	—	—

with others in the same grade. We can empirically verify these conjectures. Figure 3 shows the gender, grade, and race information in one of the five schools: students tend to befriend others of the same gender, grade, and race. Similar patterns can be observed in other schools (see Figure 7 in Appendix A). Therefore, these predictors exhibit network cohesion, explaining the differential results between our method and standard logistic regression.

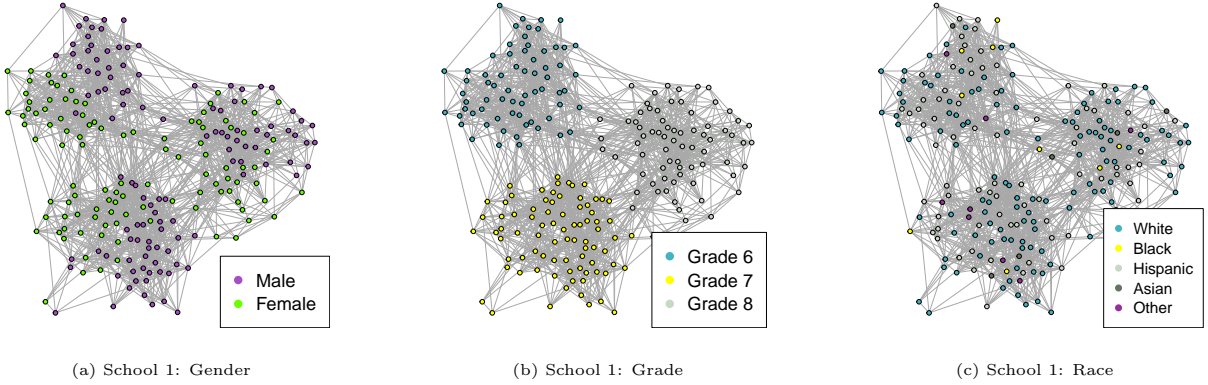


Figure 3: Friendship network of School 1, along with the corresponding gender, grade, and race information.

In summary, we have shown that social network information give important impacts in the current problem. Though both the RNC and our SP model can incorporate network information in building the logistic regression model, the available inference framework in our model provides a substantial advantage in understanding the data with more conclusive insights: both the social effect and the conflict-mitigating training are statistically significant in this example. Compared with the standard logistic regression, all the qualitative differences in estimated effects can be explained by the network cohesion phenomenon, which can be empirically verified.

All previous discussions focus on model interpretation and we have seen that differences between our model and the standard logistic regression are reasonable. Next, we use prediction performance to validate the effectiveness of our model compared with the standard logistic regression.

5.2 Predictive Model Validation

We use out-of-sample prediction performance to validate the practical significance of the network effects. Consider the scenario where the response is only partially observed. It is then useful to assess the performance of the models when they make predictions on the unobserved response variable based on the full set of covariates and the network. In particular, we use 200-fold cross-validation to assess the performance: all the students are partitioned into 200 folds randomly. We hold out one fold of the response variable and make predictions based on the fitted model from the 199 folds (with all the needed tuning). This procedure is repeated for each of the 200 folds. Since the current task is a binary classification problem, we use the ROC curves and the area under the curve (AUC) of the predicted probabilities (aggregated over the 200 iterations) as the performance metric.

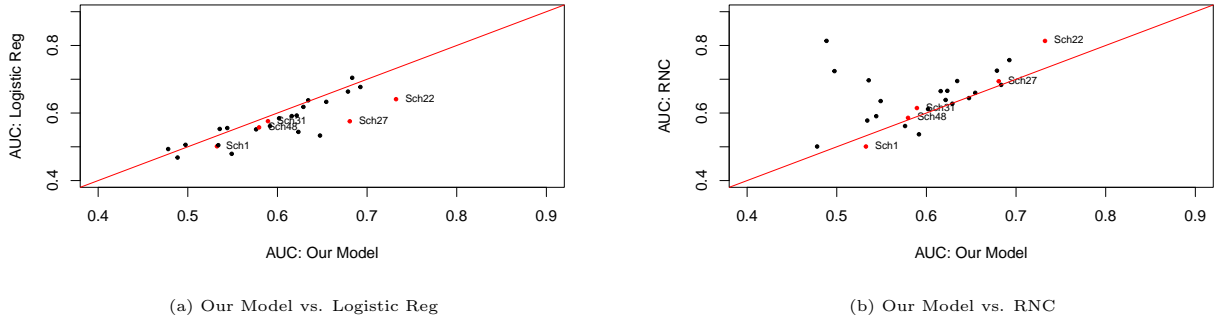


Figure 4: Prediction performance comparison for each school between our method with logistic regression and RNC.

Figure 4 shows the AUC values calculated based on predictions in each individual school by our model and the two benchmarks. The five selected schools in the previous analysis are colored red. It can be seen that overall, the RNC predictions are more accurate, and our model is also more accurate than the standard logistic regression. Due to the significant network effects of the five selected schools, our model provides more accurate predictions. The result shows that overall, the social network effects are sufficiently influential to exhibit differential prediction accuracy.

Since our prediction model interpretations in Table 7 are based on selected schools, we also want to evaluate the effects of this selection procedure. Therefore, we apply the aforementioned 200-fold cross-validation but include the school selection procedure: In each iteration, we first select five schools based on the 199 folds and then focus on model fitting and predicting the hold-out fold constrained within the selected five schools. Note that in this procedure, different schools may be selected for each iteration. Thus, this evaluation also includes the randomness of the selection. The ROC curves aggregated over the 200 folds are shown in Figure 5. The conclusion from Figure 5 is consistent with Figure 4. Both our model and the RNC effectively exploit the network information to achieve more accurate predictions. While the RNC is overall more accurate for prediction, our model's performance is not far behind.

In summary, our validation experiments show that, whether we consider the selected subset of schools or all of them, the social network effects are strong, and ignoring them results in inferior prediction performance. The RNC provides the best predictive power among the three models, but our model remains competitive. The major drawback of the RNC is the lack of an inference framework, which hinders scientific interpretations of the problem. In contrast, the proposed SP framework offers interpretations, inference, and effective predictions all in one model, with provable

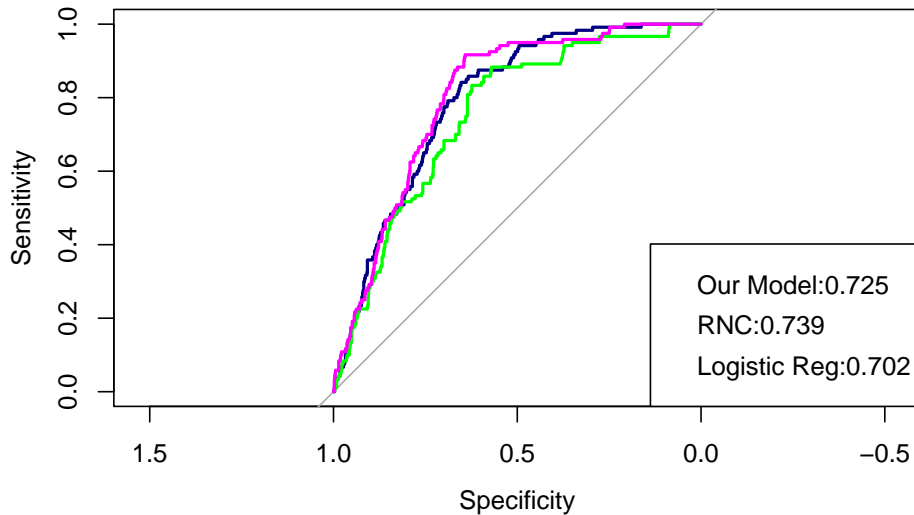


Figure 5: ROC curves of three methods restricted to selected schools from the 200-fold cross-validation procedure.

robustness to network perturbations.

6 Discussion

We have introduced a class of generalized linear models linked by network subspace assumptions. The advantage of this framework lies in its flexibility due to the nonparametric network effects, the availability of a statistical inference framework, and its proven robustness to network structure perturbations. We have empirically verified that the inference is valid for network perturbations from random network models and algorithmic perturbations from network embedding methods.

Several interesting directions for expanding our study remain. One particularly intriguing problem is incorporating more general graph neural networks [Scarselli et al., 2008, Kipf and Welling, 2016] into similar subspace models for network-linked data and extending the inference framework to such situations. In a related direction, conformal predictions have been studied for network regression problems [Lunde et al., 2023], but addressing the inference problem with these complications can be more widely useful yet more challenging. Finally, a fundamental problem is using such subspace models to handle spill-over effects of randomized experiments on social networks or even more general causal analysis with network effects [Sinclair et al., 2012, Phan and Airolidi, 2015, Lee and Ogburn, 2021, Hayes et al., 2022], or even other causal analysis involving network-mediated effects. Formulating a spill-over or mediation causal model in the subspace format would be crucial when we want to generalize the proposed framework for such analysis.

References

- M. Armillotta and K. Fokianos. Nonlinear network autoregression. *The Annals of Statistics*, 51(6): 2526–2552, 2023.
- A. Athreya, D. E. Fishkind, M. Tang, C. E. Priebe, Y. Park, J. T. Vogelstein, K. Levin, V. Lyzinski, Y. Qin, and D. L. Sussman. Statistical inference on random dot product graphs: a survey. *Journal of Machine Learning Research*, 18(226):1–92, 2018.

- P. J. Bickel and A. Chen. A nonparametric view of network models and newman–girvan and other modularities. *Proceedings of the National Academy of Sciences*, 106(50):21068–21073, 2009.
- J. H. Chang and S. Paul. Embedding network autoregression for time series analysis and causal peer effect inference. *arXiv preprint arXiv:2406.05944*, 2024.
- L. Cuadra, S. Salcedo-Sanz, J. Del Ser, S. Jiménez-Fernández, and Z. W. Geem. A critical review of robustness in power grids using complex networks concepts. *Energies*, 8(9):9211–9265, 2015.
- G. Fang, G. Xu, H. Xu, X. Zhu, and Y. Guan. Group network hawkes process. *Journal of the American Statistical Association*, pages 1–17, 2023.
- Q.-B. Gao, J.-G. Lin, C.-H. Zhu, and Y.-H. Wu. Asymptotic properties of maximum quasi-likelihood estimators in generalized linear models with adaptive designs. *Statistics*, 46(6):833–846, 2012.
- P. J. Green. Iteratively reweighted least squares for maximum likelihood estimation, and some robust and resistant alternatives. *Journal of the Royal Statistical Society: Series B (Methodological)*, 46(2):149–170, 1984.
- A. Grover and J. Leskovec. node2vec: Scalable feature learning for networks. In *Proceedings of the 22nd ACM SIGKDD International Conference on Knowledge Discovery and Data Mining*, 2016.
- X. Han, Q. Yang, and Y. Fan. Universal rank inference via residual subsampling with application to large networks. *The Annals of Statistics*, 51(3):1109–1133, 2023.
- K. M. Harris. *The National Longitudinal Study of Adolescent to Adult Health (Add Health), Waves I & II, 1994-1996; Wave III, 2001-2002; Wave IV, 2007-009 [machine-readable data file and documentation]*. Carolina Population Center, University of North Carolina at Chapel Hill, 2009.
- A. Hayes, M. M. Fredrickson, and K. Levin. Estimating network-mediated causal effects via spectral embeddings. *arXiv preprint arXiv:2212.12041*, 2022.
- Y. He, J. Sun, Y. Tian, Z. Ying, and Y. Feng. Semiparametric modeling and analysis for longitudinal network data. *arXiv preprint arXiv:2308.12227*, 2023.
- P. W. Holland, K. B. Laskey, and S. Leinhardt. Stochastic blockmodels: First steps. *Social networks*, 5(2):109–137, 1983.
- P. Holme. Modern temporal network theory: a colloquium. *The European Physical Journal B*, 88: 1–30, 2015.
- B. Karrer and M. E. Newman. Stochastic blockmodels and community structure in networks. *Physical review E*, 83(1):016107, 2011.
- T. N. Kipf and M. Welling. Semi-supervised classification with graph convolutional networks. In *International Conference on Learning Representations*, 2016.
- C. M. Le and E. Levina. Estimating the number of communities by spectral methods. *Electronic Journal of Statistics*, 16(1):3315–3342, 2022.
- C. M. Le and T. Li. Linear regression and its inference on noisy network-linked data. *Journal of the Royal Statistical Society Series B: Statistical Methodology*, 84(5):1851–1885, 2022.

- Y. Le Gat. Extending the yule process to model recurrent pipe failures in water supply networks. *Urban Water Journal*, 11(8):617–630, 2014.
- S. Y. Lee. Document vectorization method using network information of words. *PloS one*, 14(7):e0219389, 2019.
- Y. Lee and E. L. Ogburn. Network dependence can lead to spurious associations and invalid inference. *Journal of the American Statistical Association*, 116(535):1060–1074, 2021.
- T. Li and C. M. Le. Network estimation by mixing: Adaptivity and more. *Journal of the American Statistical Association*, pages 1–16, 2023.
- T. Li, E. Levina, and J. Zhu. Prediction models for network-linked data. *Annals of Applied Statistics*, 13(1):132–164, 2019.
- T. Li, E. Levina, and J. Zhu. Network cross-validation by edge sampling. *Biometrika*, 107(2):257–276, 2020.
- T. Li, E. Levina, J. Zhu, and C. M. Le. *randnet: Random Network Model Estimation, Selection and Parameter Tuning*, 2023. URL <https://CRAN.R-project.org/package=randnet>. R package version 0.7.
- J. W. Lindeberg. Eine neue herleitung des exponentialgesetzes in der wahrscheinlichkeitsrechnung. *Mathematische Zeitschrift*, 15:211–225, 1922. URL <http://eudml.org/doc/167717>.
- X. Liu and K.-W. Huang. Controlling homophily in social network regression analysis by machine learning. *INFORMS Journal on Computing*, 2024.
- R. Lunde, E. Levina, and J. Zhu. Conformal prediction for network-assisted regression. *arXiv preprint arXiv:2302.10095*, 2023.
- X. Mao, D. Chakrabarti, and P. Sarkar. Consistent nonparametric methods for network assisted covariate estimation. In *International Conference on Machine Learning*, pages 7435–7446. PMLR, 2021.
- P. McCullagh. *Generalized linear models*. Routledge, 2019.
- L. Michell and P. West. Peer pressure to smoke: the meaning depends on the method. *Health education research*, 11(1):39–49, 1996.
- L. Michell, Michael Pearson. Smoke rings: social network analysis of friendship groups, smoking and drug-taking. *Drugs: education, prevention and policy*, 7(1):21–37, 2000.
- S. Mukherjee, Z. Niu, S. Halder, B. B. Bhattacharya, and G. Michailidis. High dimensional logistic regression under network dependence. *arXiv preprint arXiv:2110.03200*, 2021.
- J.-P. Onnela, J. Saramäki, J. Hyvönen, G. Szabó, D. Lazer, K. Kaski, J. Kertész, and A.-L. Barabási. Structure and tie strengths in mobile communication networks. *Proceedings of the National Academy of Sciences*, 104(18):7332–7336, 2007.
- A. Özgür, T. Vu, G. Erkan, and D. R. Radev. Identifying gene-disease associations using centrality on a literature mined gene-interaction network. *Bioinformatics*, 24(13):i277–i285, 2008.

- E. L. Paluck, H. Shepherd, and P. M. Aronow. Changing climates of conflict: A social network experiment in 56 schools. *Proceedings of the National Academy of Sciences*, 113(3):566–571, 2016.
- B. Perozzi, R. Al-Rfou, and S. Skiena. Deepwalk: Online learning of social representations. In *Proceedings of the 20th ACM SIGKDD International Conference on Knowledge Discovery and Data Mining*, pages 701–710, 2014.
- T. Q. Phan and E. M. Airolidi. A natural experiment of social network formation and dynamics. *Proceedings of the National Academy of Sciences*, 112(21):6595–6600, 2015.
- M. Pozek, L. Sikic, P. Afric, A. S. Kurdija, K. Vladimir, G. Delac, and M. Silic. Performance of common classifiers on node2vec network representations. In *2019 42nd International Convention on Information and Communication Technology, Electronics and Microelectronics (MIPRO)*, pages 925–930. IEEE, 2019.
- K. S. Pranathi and C. Prathibhamol. Node classification through graph embedding techniques. In *2021 4th Biennial International Conference on Nascent Technologies in Engineering (ICNTE)*, pages 1–4. IEEE, 2021.
- B. Rozemberczki and R. Sarkar. Fast sequence-based embedding with diffusion graphs. In *Complex Networks IX: Proceedings of the 9th Conference on Complex Networks CompleNet 2018 9*, pages 99–107. Springer, 2018.
- B. Rozemberczki, O. Kiss, and R. Sarkar. Karate Club: An API Oriented Open-source Python Framework for Unsupervised Learning on Graphs. In *Proceedings of the 29th ACM International Conference on Information and Knowledge Management (CIKM '20)*, page 3125–3132. ACM, 2020.
- F. Scarselli, M. Gori, A. C. Tsoi, M. Hagenbuchner, and G. Monfardini. The graph neural network model. *IEEE Transactions on Neural Networks*, 20(1):61–80, 2008.
- B. Sinclair, M. McConnell, and D. P. Green. Detecting spillover effects: Design and analysis of multilevel experiments. *American Journal of Political Science*, 56(4):1055–1069, 2012.
- T. Sit and Z. Ying. Event history analysis of dynamic networks. *Biometrika*, 108(1):223–230, 2021.
- L. A. Stefanski and R. J. Carroll. Covariate measurement error in logistic regression. *The Annals of Statistics*, 13(4):1335–1351, 1985.
- L. Su, W. Lu, R. Song, and D. Huang. Testing and estimation of social network dependence with time to event data. *Journal of the American Statistical Association*, 2019.
- W. Van den Bos, E. A. Crone, R. Meuwese, and B. Güroğlu. Social network cohesion in school classes promotes prosocial behavior. *PLoS One*, 13(4):e0194656, 2018.
- W. Wu and C. Leng. A random graph-based autoregressive model for networked time series. *arXiv preprint arXiv:2309.08488*, 2023.
- C. Yin, L. Zhao, and C. Wei. Asymptotic normality and strong consistency of maximum quasi-likelihood estimates in generalized linear models. *Science in China Series A*, 49:145–157, 2006.
- H. Yu, P. Braun, M. A. Yıldırım, I. Lemmens, K. Venkatesan, J. Sahalie, T. Hirozane-Kishikawa, F. Gebreab, N. Li, N. Simonis, et al. High-quality binary protein interaction map of the yeast interactome network. *Science*, 322(5898):104–110, 2008.

- X. Zeng, L. Liu, L. Lü, and Q. Zou. Prediction of potential disease-associated micrnas using structural perturbation method. *Bioinformatics*, 34(14):2425–2432, 2018.
- X. Zhang, R. Pan, G. Guan, X. Zhu, and H. Wang. Logistic regression with network structure. *Statistica Sinica*, 30(2):673–693, 2020.
- Y. Zhang and M. Tang. A theoretical analysis of deepwalk and node2vec for exact recovery of community structures in stochastic blockmodels. *IEEE Transactions on Pattern Analysis and Machine Intelligence*, 2023.
- Y. Zhang, E. Levina, and J. Zhu. Community detection in networks with node features. *Electronic Journal of Statistics*, 10(2):3153–3178, 2016.
- Y. Zhang, E. Levina, and J. Zhu. Estimating network edge probabilities by neighbourhood smoothing. *Biometrika*, 104(4):771–783, 2017.
- X. Zhu, R. Pan, G. Li, Y. Liu, and H. Wang. Network vector autoregression. *The Annals of Statistics*, 45(3):1096–1123, 2017.

A Additional results of the school conflict analysis

A.1 Finalized model on all 25 schools

The estimated parameters and p-values (after variable selection by backward elimination) using the averaged network of two waves in all schools are summarized in Table 8. Under our model, r is detected to be 0, and the χ^2 test for the existence of the network effect yields a p-value $< 10^{-8}$, suggesting the statistical significance of the network information.

Table 8: Estimated coefficients and p-values of our model, standard logistic regression and RNC using the average network of two waves involving all schools.

	Our Model		Logistic Reg		RNC	
	coef.	p-value	coef.	p-value	coef.	p-value
Gender:Male	-0.443	$< 10^{-3}$	-0.419	$< 10^{-3}$	-0.517	–
Grade	-0.323	$< 10^{-3}$	-0.256	$< 10^{-3}$	-0.484	–
Friends like House					0.087	–
Home Language	0.272	$< 10^{-3}$	0.324	$< 10^{-3}$	0.197	–
Treatment	0.837	$< 10^{-3}$	0.820	$< 10^{-3}$	0.804	–
GPA					-0.153	–
Influencer					0.349	–
Race:White					-0.247	–
Race:Black					-0.071	–
Race:Hispanic					-0.203	–
Race:Asian					0.026	–

A.2 Robustness validation with three network constructions

Table 9: Estimated coefficients and p-values of our model using three different versions of the friendship networks. The blanks indicate that the variables are removed in the backward elimination procedure.

	Wave Average		Wave I		Wave II	
	coef.	p-value	coef.	p-value	coef.	p-value
Gender:Male	-0.443	$< 10^{-3}$	-0.429	$< 10^{-3}$	-0.427	$< 10^{-3}$
Grade	-0.323	$< 10^{-3}$	-0.252	$< 10^{-3}$	-0.257	$< 10^{-3}$
Friends like House						
Home Language	0.272	$< 10^{-3}$	0.316	$< 10^{-3}$	0.366	$< 10^{-3}$
Treatment	0.837	$< 10^{-3}$	0.842	$< 10^{-3}$	0.851	$< 10^{-3}$
GPA						
Influencer						
Race:White						
Race:Black						
Race:Hispanic						
Race:Asian						

To evaluate the robustness of our inference results to network perturbations, we fit our model separately using the Wave I and Wave II networks. In Table 9, we present the results of the same analysis with backward elimination, showing the estimated parameters and p-values for the models based on the three versions of the networks. Despite the significant variations in the networks at the edge level (Figure 1), our method consistently selects the same set of variables, with only minor

numerical differences across all three versions. These findings demonstrate the robustness of our framework. As noted in [Le and Li \[2022\]](#), this stability arises because, although the individual edges in the friendship networks experienced substantial changes, the overall spectral structure of the adjacency matrices remained stable.

A.3 Predictive comparisons with embedding-based methods

We have also evaluated the possibility of using deep-learning-based embedding methods to incorporate the network information, as discussed in [Section 4.2](#). [Figure 6](#) shows the predictive AUC of the fitted models based on embedded similarity relations from DeepWalk, Node2Vec, and Diff2Vec, compared with the fitted model based on the observed network structure. The evaluation follows the same procedure described in [Section 5](#). It can be seen that the relational data learned from the embedding methods do not lead to better predictive performance. This may indicate that the relevant relational information in the current problem is already reflected in the observed adjacency matrix, and the additional nonlinear transformations introduced by these embedding methods do not provide further benefits.

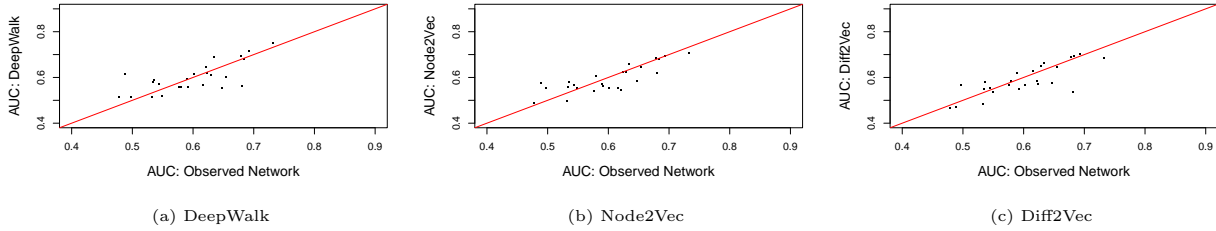


Figure 6: Prediction performance comparison for each school between using the observed network (Wave I + Wave II), and the embedding similarity of DeepWalk, Node2Vec and Diff2Vec.

A.4 Covariate correlation with network structures in the refined analysis

[Figure 7](#) displays the gender, grade and race information on the other four selected schools in our refined analysis. These covariates displays evident cohesive pattern based on the network structure, which explains why the inference can be different for them between our model and the logistic regression without using the network information.

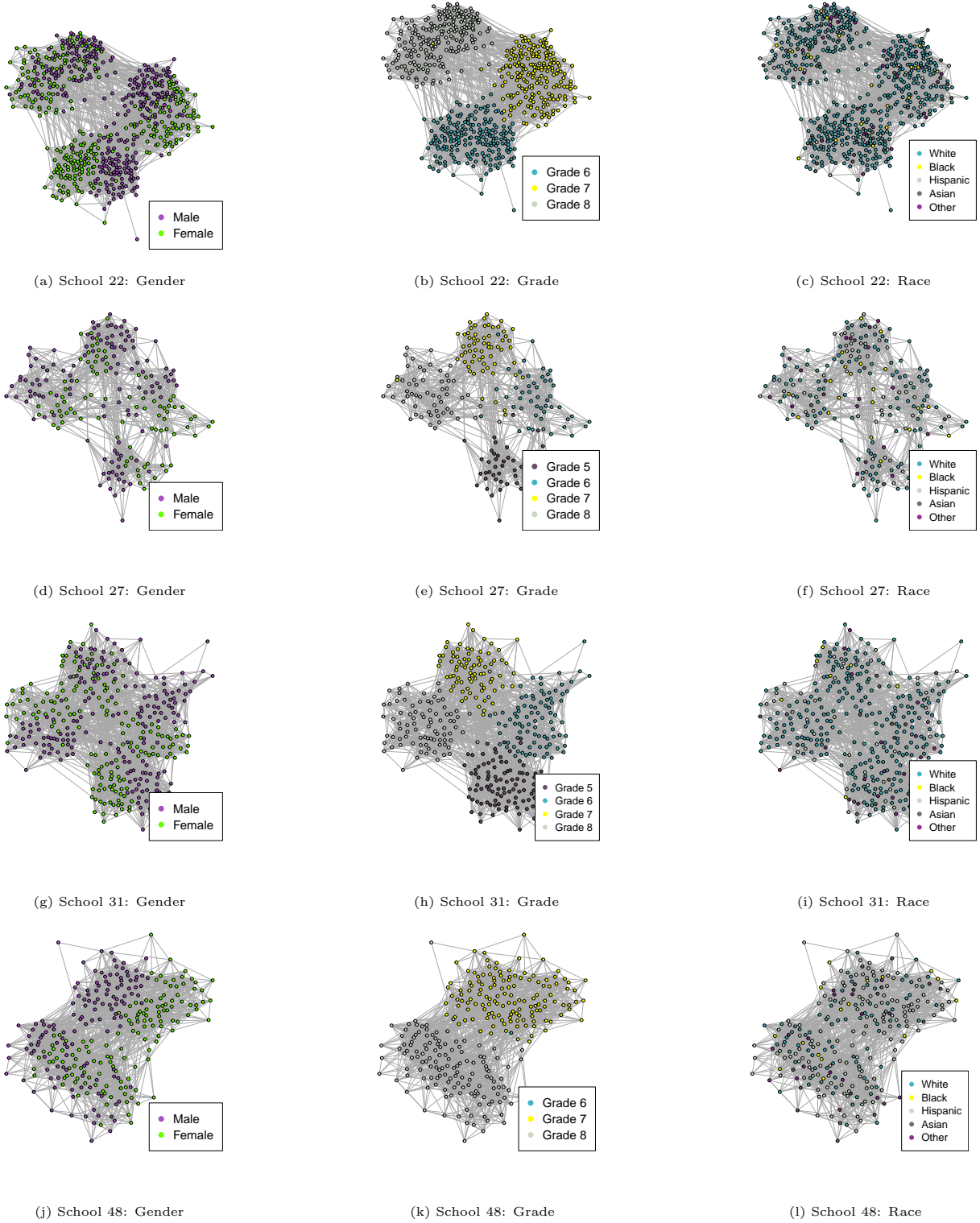


Figure 7: Friendship networks of four schools, along with the corresponding gender, grade, and race information.

B Proofs for theoretical results

Before proving our main results in subsequent appendices, let us gather here some important properties for the subspace estimators $\hat{\mathcal{R}}$, $\hat{\mathcal{C}}$, and $\hat{\mathcal{N}}$ in (15). Similar to Le and Li [2022], we will show that these estimators are sufficiently close to \mathcal{R} , \mathcal{C} and \mathcal{N} , respectively, which are defined in Section 2.3. Instead of studying these subspaces directly, we will work with the orthogonal projections onto them. To this end, denote

$$\mathcal{P}_R = n^{-1} Z_{1:r} Z_{1:r}^\top, \quad \mathcal{P}_C = n^{-1} Z_{(r+1):p} Z_{(r+1):p}^\top, \quad \mathcal{P}_N = n^{-1} W_{(r+1):K} W_{(r+1):K}^\top.$$

Similarly, denote

$$\hat{\mathcal{P}}_R = n^{-1} \tilde{Z}_{1:r} \tilde{Z}_{1:r}^\top, \quad \hat{\mathcal{P}}_C = n^{-1} \tilde{Z}_{(r+1):p} \tilde{Z}_{(r+1):p}^\top, \quad \hat{\mathcal{P}}_N = n^{-1} \tilde{W}_{(r+1):K} \tilde{W}_{(r+1):K}^\top.$$

We first recall Corollary 5 in Le and Li [2022], which provides an error bound for the subspace estimation.

Proposition 1 (Subspace perturbation). *Assume that Assumption 5 holds. There exists a constant $C_1 > 0$ such that,*

$$\max \left\{ \|\hat{\mathcal{P}}_R - \mathcal{P}_R\|, \|\hat{\mathcal{P}}_C - \mathcal{P}_C\|, \|\hat{\mathcal{P}}_N - \mathcal{P}_N\| \right\} \leq C_1 \bar{\tau}_n,$$

where

$$\bar{\tau}_n = \frac{n^{-3/2} \|(\tilde{W} \tilde{W}^\top - W W^\top) Z\|}{\min \left\{ (1 - \sigma_{r+1})^3, \sigma_{r+s}^3 \right\}}, \quad (25)$$

and the singular values σ_{r+1} and σ_{r+s} are defined in (6).

Recall the “new covariate” vectors g_i and \tilde{g}_i , defined in Section 2.3, which combine the covariate and relational information for node i :

$$g_i = (Z_{i,1:p} \ W_{i,(r+1):K})^\top, \quad \tilde{g}_i = (\tilde{Z}_{i,1:p} \ \tilde{W}_{i,(r+1):K})^\top.$$

These vectors depend on the choices of bases for $\text{col}(X)$, $S_K(P)$, and $S_K(\hat{P})$ through Z , W , \tilde{Z} and \tilde{W} . Due to the nature of these choices, g_i and \tilde{g}_i can be approximately aligned through an almost rotation matrix defined by

$$T_n := \begin{pmatrix} \tilde{Z}_{1:r}^\top Z_{1:r}/n & 0 & 0 \\ 0 & \tilde{Z}_{(r+1):p}^\top Z_{(r+1):p}/n & 0 \\ 0 & 0 & \tilde{W}_{(r+1):K}^\top W_{(r+1):K}/n \end{pmatrix}. \quad (26)$$

Using Proposition 1, we now bound the error of this alignment.

Lemma 1 (Covariate alignment). *Suppose that Assumption 5 holds. Then there exists a constant $C_2 > 0$,*

$$\|g_i - T_n^\top \tilde{g}_i\| \leq C_2 n^{1/2} \bar{\tau}_n, \quad (27)$$

$$n^{-1} \sum_{i=1}^n \|g_i - T_n^\top \tilde{g}_i\| \leq C_2 \bar{\tau}_n, \quad (28)$$

$$\|T_n^\top T_n - I_{K+p-r}\|_\infty \leq C_2 \bar{\tau}_n. \quad (29)$$

Proof of Lemma 1. We first prove (27). Since the norm of a vector is always bounded by the sum of the norms of its blocks, we have

$$\begin{aligned} \|g_i - T_n^\top \tilde{g}_i\| &\leq \|Z_{i,1:r}^\top - n^{-1} Z_{1:r}^\top \tilde{Z}_{1:r} \tilde{Z}_{i,1:r}^\top\| \\ &+ \|Z_{i,(r+1):p}^\top - n^{-1} Z_{(r+1):p}^\top \tilde{Z}_{(r+1):p} \tilde{Z}_{i,(r+1):p}^\top\| \\ &+ \|W_{i,(r+1):K}^\top - n^{-1} W_{(r+1):K}^\top \tilde{W}_{(r+1):K} \tilde{W}_{i,(r+1):K}^\top\|. \end{aligned} \quad (30)$$

We will prove that each term on the right-hand side of the above inequality is of order $O(n^{1/2} \bar{\tau}_n)$. For the first term, since columns of $Z_{1:r}$ are of norm \sqrt{n} , by Proposition 1,

$$\begin{aligned} \|Z_{i,1:r}^\top - n^{-1} Z_{1:r}^\top \tilde{Z}_{1:r} \tilde{Z}_{i,1:r}^\top\| &= \|Z_{i,1:r} - n^{-1} \tilde{Z}_{i,1:r} \tilde{Z}_{1:r}^\top Z_{1:r}\| \leq \|Z_{1:r} - n^{-1} \tilde{Z}_{1:r} \tilde{Z}_{1:r}^\top Z_{1:r}\|_F \\ &= \|(I_r - n^{-1} \tilde{Z}_{1:r} \tilde{Z}_{1:r}^\top) Z_{1:r}\|_F \\ &= \|n^{-1} (Z_{1:r} Z_{1:r}^\top - \tilde{Z}_{1:r} \tilde{Z}_{1:r}^\top) Z_{1:r}\|_F = \|(\hat{\mathcal{P}}_R - \mathcal{P}_R) Z_{1:r}\|_F \\ &\leq \sum_{i=1}^r \|(\hat{\mathcal{P}}_R - \mathcal{P}_R) Z_i\| \leq C_1 r n^{1/2} \bar{\tau}_n. \end{aligned}$$

Similarly, for the second term on the right-hand side of (30), we have

$$\|Z_{i,(r+1):p}^\top - n^{-1} Z_{(r+1):p}^\top \tilde{Z}_{(r+1):p} \tilde{Z}_{i,(r+1):p}^\top\| \leq \sum_{i=1}^{p-r} \|(\hat{\mathcal{P}}_C - \mathcal{P}_C) Z_{r+i}\| \leq C_1 (p-r) n^{1/2} \bar{\tau}_n.$$

And for the last term on the right-hand side of (30),

$$\begin{aligned} \|W_{i,(r+1):K}^\top - n^{-1} W_{(r+1):K}^\top \tilde{W}_{(r+1):K} \tilde{W}_{i,(r+1):K}^\top\| &\leq \sum_{i=1}^{K-r} \|(\hat{\mathcal{P}}_N - \mathcal{P}_N) W_{r+i}\| \\ &\leq C_1 (K-r) n^{1/2} \bar{\tau}_n. \end{aligned}$$

These three inequalities imply (27).

We now prove (28). Summing inequality (30) over i from 1 to n , we get

$$\begin{aligned} \sum_{i=1}^n \|g_i - T_n^\top \tilde{g}_i\| &\leq \sum_{i=1}^n \|Z_{i,1:r}^\top - n^{-1} Z_{1:r}^\top \tilde{Z}_{1:r} \tilde{Z}_{i,1:r}^\top\| \\ &+ \sum_{i=1}^n \|Z_{i,(r+1):p}^\top - n^{-1} Z_{(r+1):p}^\top \tilde{Z}_{(r+1):p} \tilde{Z}_{i,(r+1):p}^\top\| \\ &+ \sum_{i=1}^n \|W_{i,(r+1):K}^\top - n^{-1} W_{(r+1):K}^\top \tilde{W}_{(r+1):K} \tilde{W}_{i,(r+1):K}^\top\|. \end{aligned} \quad (31)$$

As before, we will show that each sum on the right-hand side of (31) is of order $O(\bar{\tau}_n)$. Regarding

the first sum, by the Cauchy-Schwartz inequality and Proposition 1,

$$\begin{aligned}
\sum_{i=1}^n \left\| Z_{i,1:r}^\top - n^{-1} Z_{1:r}^\top \tilde{Z}_{1:r} \tilde{Z}_{i,1:r}^\top \right\| &= \sum_{i=1}^n \left\| Z_{i,1:r} - n^{-1} \tilde{Z}_{i,1:r} \tilde{Z}_{1:r}^\top Z_{1:r} \right\| \\
&\leq n^{1/2} \left\| Z_{1:r} - n^{-1} \tilde{Z}_{1:r} \tilde{Z}_{1:r}^\top Z_{1:r} \right\|_F \\
&= n^{1/2} \left\| \left(I_r - n^{-1} \tilde{Z}_{1:r} \tilde{Z}_{1:r}^\top \right) Z_{1:r} \right\|_F \\
&= n^{1/2} \left\| n^{-1} \left(Z_{1:r} Z_{1:r}^\top - \tilde{Z}_{1:r} \tilde{Z}_{1:r}^\top \right) Z_{1:r} \right\|_F \\
&= n^{1/2} \left\| (\hat{\mathcal{P}}_R - \mathcal{P}_R) Z_{1:r} \right\|_F \\
&\leq n^{1/2} \sum_{i=1}^r \left\| (\hat{\mathcal{P}}_R - \mathcal{P}_R) Z_i \right\| \leq C_1 r n \bar{\tau}_n.
\end{aligned}$$

Similarly, the second sum and the third sum on the right-hand side of (31) are bounded by $C_1(p-r)n\bar{\tau}_n$ and $C_1(K-r)n\bar{\tau}_n$, respectively. These inequalities and (31) then imply (28).

Finally, we prove (29). Since T_n is a block-diagonal matrix with three non-zero blocks on the diagonal, $T_n^\top T_n - I_{K+p-r}$ is also block-diagonal with three non-zero blocks on the diagonal given by:

$$\begin{aligned}
&n^{-2} Z_{1:r}^\top \tilde{Z}_{1:r} \tilde{Z}_{1:r}^\top Z_{1:r} - I_r, \\
&n^{-2} Z_{(r+1):p}^\top \tilde{Z}_{(r+1):p} \tilde{Z}_{(r+1):p}^\top Z_{(r+1):p} - I_{p-r}, \\
&n^{-2} W_{(r+1):K}^\top \tilde{W}_{(r+1):K} \tilde{W}_{(r+1):K}^\top W_{(r+1):K} - I_{K-r}.
\end{aligned}$$

We will show that each diagonal block is of order $O(\bar{\tau}_n)$. Regarding the first block, for any unit vectors $u, v \in \mathbb{R}^{k-r}$, by Proposition 1 we have

$$\begin{aligned}
u^\top \left(Z_{1:r}^\top \tilde{Z}_{1:r} \tilde{Z}_{1:r}^\top Z_{1:r} - n^2 I_r \right) v &= u^\top Z_{1:r}^\top \left(\tilde{Z}_{1:r} \tilde{Z}_{1:r}^\top - Z_{1:r} Z_{1:r}^\top \right) Z_{1:r} v \\
&\leq \|Z_{1:r} u\| \left\| \tilde{Z}_{1:r} \tilde{Z}_{1:r}^\top - Z_{1:r} Z_{1:r}^\top \right\| \|Z_{1:r} v\| \\
&= n \|Z_{1:r} u\| \left\| \mathcal{P}_C - \hat{\mathcal{P}}_C \right\| \|Z_{1:r} v\| \\
&\leq C_1 n \bar{\tau}_n \|Z_{1:r} u\| \|Z_{1:r} v\|.
\end{aligned}$$

Since columns of $Z_{1:r}$ are of norm $n^{1/2}$, it follows that $\|Z_{1:r} u\| \|Z_{1:r} v\| \leq rn$. Because u and v are arbitrary, this implies the infinity norm of the first diagonal block is at most $C_1 r n^2 \bar{\tau}_n$. The same argument can be applied to the second and third diagonal blocks to show that their infinity norms are bounded by $C_1(p-r)n^2 \bar{\tau}_n$ and $C_1(K-r)n^2 \bar{\tau}_n$, respectively. Together, these bounds imply (29) and the proof of Lemma 1 is complete. \square

Then we show an additional Lemma aims to bound the T_n 's eigenvalues that will be applied repeatedly in the proof of main theorems.

Corollary 4 (Eigenvalue bound of T_n). *Suppose that Assumption 5 holds. Then with the same constant C_2 from Lemma 1*

$$1 - C_2 \bar{\tau}_n \leq \lambda_{\min}^2(T_n) \leq \lambda_{\max}^2(T_n) \leq 1 + C_2 \bar{\tau}_n, \quad (32)$$

for sufficiently large n

Proof of Corollary 4. Based on Lemma 1, T_n is nonsingular when $\bar{\tau}_n < 1/C_2$. Then we try to bound T_n 's eigenvalue λ by bound $\|T_n u_\lambda\|$, where $\lambda u_\lambda = T_n u_\lambda$ and $u_\lambda \in \mathbb{R}^{K+p-r}$ is a unit vector. By infinity norm bound (29) in Lemma 1

$$\begin{aligned} |\lambda^2 - 1| &= \left| \|T_n u_\lambda\|^2 - 1 \right| = u_\lambda^\top T_n^\top T_n u_\lambda - 1 = u_\lambda^\top (T_n^\top T_n - I_{K+p-r}) u_\lambda \\ &\leq \|T_n^\top T_n - I_{K+p-r}\| \leq \|T_n^\top T_n - I_{K+p-r}\|_\infty \leq C_2 \bar{\tau}_n. \end{aligned}$$

Therefore,

$$1 - C_2 \bar{\tau}_n \leq \lambda^2 \leq 1 + C_2 \bar{\tau}_n.$$

Since λ can be any eigenvalue of T_n , we have proved (32). \square

C The Proof of Theorem 1

We proceed to prove Theorem 1 about the existence and consistency of the proposed estimates. Overall, we follow the proof strategy for generalized linear models with fixed design Yin et al. [2006]. The main difference between our proof and the proof in Yin et al. [2006] is that the combinations of covariate and relational information for all the nodes, denoted by \tilde{g}_i , are not exactly observed. Therefore, we need to carefully track down the measurement errors. To prove Theorem 1, we begin with the following remarks and lemmas.

Remark 1. Assumption 1 implies that γ^* is bounded because

$$\|\gamma^*\| = n^{-1/2} \|W\gamma^*\| = n^{-1/2} \|X\beta^* + X\theta^* + \alpha^*\| \leq n^{-1/2} (\|X\beta^*\| + \|X\theta^*\| + \|\alpha^*\|) \leq 3C.$$

Remark 2. Denote $\eta := h'/v : \mathbb{R} \rightarrow \mathbb{R}$. Then there exists a constant $M > 0$, when $|t| \leq 12C^2$, the absolute value of function $h(t), v(t), \eta(t), \eta(t)h(t), \eta(t)h'(t)$ and their first and second derivatives are all bounded by M because every real-valued continuous function on a compact set is necessarily bounded.

Lemma 2 (Lemma 3 in Yin et al. [2006]). Let $\varphi : \mathbb{R}^m \rightarrow \mathbb{R}^m$ be a smooth injective map with $\varphi(x^*) = y^*$ and for some $\rho, \delta > 0$,

$$\min_{\|x - x^*\| = \delta} \|\varphi(x) - y^*\| \geq \rho.$$

Then for any y with $\|y - y^*\| \leq \rho$, there exists x with $\|x - x^*\| \leq \delta$ such that $\varphi(x) = y$.

Lemma 3. Assume that Assumptions 1 to 5 hold. For a constant $\delta_0 > 0$, denote

$$N_n(\delta_0) = \left\{ \gamma : \|T_n^{-1}\gamma - \gamma^*\| \leq \delta_0 n^{-1/2} \right\}.$$

Then there exists a constant $c > 0$ such that for any $\varepsilon > 0$ and sufficiently large n , with probability at least $1 - \varepsilon$,

$$\inf_{\gamma \in \partial N_n(\delta_0)} \left\| T_n^\top \tilde{S}(\gamma) - T_n^\top \tilde{S}(T_n \gamma^*) \right\| \geq cn^{-1/2}, \quad (33)$$

$$\left\| T_n^\top \tilde{S}(T_n \gamma^*) \right\| \leq cn^{-1/2}. \quad (34)$$

This lemma is crucial for proving Theorem 1. Its proof is given in Appendix D.

Proof of Theorem 1. We first prove (18). Instead of working with the sample score function $\tilde{S}(\gamma)$ directly, it will be more convenient to scale it and work with

$$L(\gamma) := T_n^\top \tilde{S}(T_n \gamma).$$

The estimating equation $\tilde{S}(\gamma) = 0$ is equivalent to

$$L(T_n^{-1} \gamma) - L(\gamma^*) = -L(\gamma^*).$$

To prove (18), we apply Lemma 2 with $\varphi(x) = L(x) - L(\gamma^*)$, $x^* = \gamma^*$, and $y^* = 0$. According to this lemma, for $y = -L(\gamma^*)$ with $\|y - y^*\| = \|L(\gamma^*)\| =: \rho$, there exists $x = T_n^{-1} \gamma$ with $\gamma := T_n x$ and $\|x - x^*\| = \|T_n^{-1} \gamma - \gamma^*\| \leq \delta$ such that $\varphi(x) = y$, or equivalently $\tilde{S}(\gamma) = 0$. We need to specify δ such that the following condition of the lemma holds:

$$\min_{\|x - x^*\| = \delta} \|\varphi(x) - y^*\| = \min_{\|T_n^{-1} \gamma - \gamma^*\| = \delta} \|L(T_n^{-1} \gamma) - L(\gamma^*)\| \geq \rho.$$

For consistency of $\gamma = T_n x$ such that $\tilde{S}(\gamma) = 0$, we choose $\delta = \delta_0 n^{-1/2}$ for some δ_0 and denote

$$N_n(\delta_0) = \left\{ \gamma : \|T_n^{-1} \gamma - \gamma^*\| \leq \delta_0 n^{-1/2} \right\}. \quad (35)$$

By combining (33) and (34) in Lemma 3, we obtain that with probability at least $1 - \varepsilon$,

$$\min_{\gamma \in \partial N_n(\delta_0)} \|L(T_n^{-1} \gamma) - L(\gamma^*)\| \geq \|L(\gamma^*)\| = \rho.$$

The proof of (18) is complete.

We now prove (19), starting with the consistency of $\hat{\alpha}$. By Proposition 1 and Lemma 1,

$$\begin{aligned} \|\hat{\alpha} - \alpha^*\| &= \left\| \tilde{W}_{(r+1):K} \hat{\gamma}_{(p+1):(p+K-r)} - W_{(r+1):K} \gamma_{(p+1):(p+K-r)}^* \right\| \\ &\leq \left\| \tilde{W}_{(r+1):K} \left(\hat{\gamma}_{(p+1):(p+K-r)} - \left[\tilde{W}_{(r+1):K}^\top W_{(r+1):K} / n \right] \gamma_{(p+1):(p+K-r)}^* \right) \right\| \\ &\quad + \left\| \left(\tilde{W}_{(r+1):K} \tilde{W}_{(r+1):K}^\top W_{(r+1):K} / n - W_{(r+1):K} \right) \gamma_{(p+1):(p+K-r)}^* \right\| \\ &= n^{1/2} \left\| \hat{\gamma}_{(p+1):(p+K-r)} - \left[\tilde{W}_{(r+1):K}^\top W_{(r+1):K} / n \right] \gamma_{(p+1):(p+K-r)}^* \right\| \\ &\quad + n^{-1} \left\| \left(\tilde{W}_{(r+1):K} \tilde{W}_{(r+1):K}^\top - W_{(r+1):K} W_{(r+1):K}^\top \right) W_{(r+1):K} \gamma_{(p+1):(p+K-r)}^* \right\| \\ &= n^{1/2} \left\| \tilde{W}_{(r+1):K}^\top W_{(r+1):K} / n \left(\left(\tilde{W}_{(r+1):K}^\top W_{(r+1):K} / n \right)^{-1} \hat{\gamma}_{(p+1):(p+K-r)} - \gamma_{(p+1):(p+K-r)}^* \right) \right\| \\ &\quad + \left\| \left(\hat{\mathcal{P}}_N - \mathcal{P}_N \right) \alpha^* \right\| \\ &\leq n^{-1/2} \left\| \tilde{W}_{(r+1):K} \right\| \left\| W_{(r+1):K} \right\| \left\| \left(\tilde{W}_{(r+1):K}^\top W_{(r+1):K} / n \right)^{-1} \hat{\gamma}_{(p+1):(p+K-r)} - \gamma_{(p+1):(p+K-r)}^* \right\| \\ &\quad + \left\| \left(\hat{\mathcal{P}}_N - \mathcal{P}_N \right) \alpha^* \right\| \\ &\leq n^{1/2} \|T_n^{-1} \hat{\gamma} - \gamma^*\| + \left\| \left(\hat{\mathcal{P}}_N - \mathcal{P}_N \right) \alpha^* \right\| \\ &\leq o_p(n^{1/2}) + n^{1/2} C_2 C \bar{\tau}_n \\ &= o_p(n^{1/2}). \end{aligned}$$

We now prove the consistency for $\hat{\beta}$. Following the above argument for the bound of $\hat{\alpha}$, we obtain $\|X(\hat{\beta} - \beta^*)\| = o_p(n^{1/2})$.

$$\begin{aligned}
\|X(\hat{\beta} - \beta^*)\| &= \|\tilde{Z}_{(r+1):p}\hat{\gamma}_{(r+1):p} - Z_{(r+1):p}\gamma_{(r+1):p}^*\| \\
&\leq \|\tilde{Z}_{(r+1):p}\left(\hat{\gamma}_{(r+1):p} - \left[\tilde{Z}_{(r+1):p}^\top Z_{(r+1):p}/n\right]\gamma_{(r+1):p}^*\right)\| \\
&\leq n^{-1/2}\|\tilde{Z}_{(r+1):p}\|\|Z_{(r+1):p}\|\left\|\left(\tilde{Z}_{(r+1):p}^\top Z_{(r+1):p}/n\right)^{-1}\hat{\gamma}_{(r+1):p} - \gamma_{(r+1):p}^*\right\| \\
&\quad + \left\|\left(\hat{\mathcal{P}}_C - \mathcal{P}_C\right)\alpha^*\right\| \\
&\leq n^{1/2}\|T_n^{-1}\hat{\gamma} - \gamma^*\| + \left\|\left(\hat{\mathcal{P}}_C - \mathcal{P}_C\right)\alpha^*\right\| \\
&\leq o_p(n^{1/2}) + n^{1/2}C_2C\bar{\tau}_n \\
&= o_p(n^{1/2}).
\end{aligned}$$

Denote $u = \|\hat{\beta} - \beta^*\|^{-1}(\hat{\beta} - \beta^*)$. By the definition of $G = (X^\top X/n)^{-1}$ in Assumption 2,

$$\|\hat{\beta} - \beta^*\|^2 \left(u^\top G^{-1}u\right) = \left(\hat{\beta} - \beta^*\right)^\top G^{-1} \left(\hat{\beta} - \beta^*\right) = n^{-1}\|X(\hat{\beta} - \beta^*)\|^2.$$

Therefore by Assumption 2,

$$\|\hat{\beta} - \beta^*\| = n^{-1/2} \left(u^\top G^{-1}u\right)^{-1/2} \|X(\hat{\beta} - \beta^*)\| \leq n^{-1/2}\lambda_{\min}^{-1/2}(G)\|X(\hat{\beta} - \beta^*)\| = o_p(1).$$

For the consistency of $\hat{\theta}$,

$$\begin{aligned}
\|X(\hat{\theta} - \theta^*)\| &= \|\tilde{Z}_{1:r}\hat{\gamma}_{1:r} - Z_{1:r}\gamma_{1:r}^*\| \\
&\leq \|\tilde{Z}_{1:r}\left(\hat{\gamma}_{1:r} - \left[\tilde{Z}_{1:r}^\top Z_{1:r}/n\right]\gamma_{1:r}^*\right)\| \\
&\leq n^{-1/2}\|\tilde{Z}_{1:r}\|\|Z_{1:r}\|\left\|\left(\tilde{Z}_{1:r}^\top Z_{1:r}/n\right)^{-1}\hat{\gamma}_{1:r} - \gamma_{1:r}^*\right\| \\
&\quad + \left\|\left(\hat{\mathcal{P}}_C - \mathcal{P}_C\right)\alpha^*\right\| \\
&\leq n^{1/2}\|T_n^{-1}\hat{\gamma} - \gamma^*\| + \left\|\left(\hat{\mathcal{P}}_C - \mathcal{P}_C\right)\alpha^*\right\| \\
&\leq o_p(n^{1/2}) + n^{1/2}C_2C\bar{\tau}_n \\
&= o_p(n^{1/2}).
\end{aligned}$$

Denote $u = \|\hat{\theta} - \theta^*\|^{-1}(\hat{\theta} - \theta^*)$. Similar to the consistency of $\hat{\theta}$, by the definition of $G = (X^\top X/n)^{-1}$ in Assumption 2,

$$\|\hat{\theta} - \theta^*\| = n^{-1/2} \left(u^\top G^{-1}u\right)^{-1/2} \|X(\hat{\theta} - \theta^*)\| \leq n^{-1/2}\lambda_{\min}^{-1/2}(G)\|X(\hat{\theta} - \theta^*)\| = o_p(1).$$

□

D Proof of Lemma 3

The proof of Lemma 3 follows from several technical lemmas in this section. Recall matrix T_n from (26) and $T_n^\top \tilde{g}_i \approx g_i$ by Lemma 1. The next lemma is a consequence of the Mean Value Theorem and will be used repeatedly.

Lemma 4 (Covariate alignment). *Assume that Assumptions 1, 3 and 5 hold. Let $\eta : \mathbb{R} \rightarrow \mathbb{R}$ be a function with continuous derivative. Then*

$$\left\| T_n^\top \tilde{g}_i \eta(\tilde{g}_i^\top T_n \gamma) - g_i \eta(g_i^\top \gamma) \right\| \leq \left(2C \|\gamma\| \sup_{|t| \leq 2C \|\gamma\|} |\eta'(t)| + \sup_{|t| \leq C \|\gamma\|} |\eta(t)| \right) \|g_i - T_n^\top \tilde{g}_i\|,$$

for sufficiently large n .

Proof of Lemma 4. By triangle inequality,

$$\begin{aligned} \left\| T_n^\top \tilde{g}_i \eta(\tilde{g}_i^\top T_n \gamma) - g_i \eta(g_i^\top \gamma) \right\| &\leq \left\| T_n^\top \tilde{g}_i \left(\eta(\tilde{g}_i^\top T_n \gamma) - \eta(g_i^\top \gamma) \right) \right\| + \left\| (T_n^\top \tilde{g}_i - g_i) \eta(g_i^\top \gamma) \right\| \\ &\leq \left\| T_n^\top \tilde{g}_i \right\| \left| \eta(\tilde{g}_i^\top T_n \gamma) - \eta(g_i^\top \gamma) \right| + \left\| T_n^\top \tilde{g}_i - g_i \right\| |\eta(g_i^\top \gamma)|. \end{aligned}$$

By Assumption 1, we have $|g_i^\top \gamma| \leq \|g_i\| \|\gamma\| \leq C \|\gamma\|$, which implies

$$|\eta(g_i^\top \gamma)| \leq \sup_{|t| \leq C \|\gamma\|} |\eta(t)|.$$

We will use the Mean Value Theorem to bound $|\eta(\tilde{g}_i^\top T_n \gamma) - \eta(g_i^\top \gamma)|$. Denote

$$h(t) = \eta \left(\tilde{g}_i^\top T_n \gamma + t \left[g_i^\top \gamma - \tilde{g}_i^\top T_n \gamma \right] \right) : \mathbb{R} \rightarrow \mathbb{R}.$$

By the Mean Value Theorem, there exists $t^* \in [0, 1]$ and $z_i = \tilde{g}_i^\top T_n \gamma + t^* [g_i^\top \gamma - \tilde{g}_i^\top T_n \gamma]$ such that

$$\begin{aligned} \left| \eta(\tilde{g}_i^\top T_n \gamma) - \eta(g_i^\top \gamma) \right| &= |h(1) - h(0)| = |h'(t^*)| = |\eta'(z_i)| \left| g_i^\top \gamma - \tilde{g}_i^\top T_n \gamma \right| \\ &\leq \|g_i - T_n^\top \tilde{g}_i\| \|\gamma\| |\eta'(z_i)|. \end{aligned}$$

By the triangle inequality,

$$|z_i| = |(1 - t^*) \tilde{g}_i^\top T_n \gamma + t^* g_i^\top \gamma| \leq \max\{\|\tilde{g}_i^\top T_n\|, \|g_i\|\} \cdot \|\gamma\|.$$

By Assumption 1, we have $\|g_i\| \leq C$. In addition, by Assumptions 3, 5, and Lemma 1,

$$\left\| T_n^\top \tilde{g}_i \right\| \leq \left\| T_n^\top \tilde{g}_i - g_i \right\| + \|g_i\| \leq C_2 n^{1/2} \bar{\tau}_n + C \leq 2C, \quad (36)$$

when n is big enough. It follows that $|\eta'(z_i)| \leq \sup_{|t| \leq 2C \|\gamma\|} \|\eta'(t)\|$. Putting these inequalities together, we get

$$\left\| T_n^\top \tilde{g}_i \eta(\tilde{g}_i^\top T_n \gamma) - g_i \eta(g_i^\top \gamma) \right\| \leq \left(2C \|\gamma\| \sup_{|t| \leq 2C \|\gamma\|} |\eta'(t)| + \sup_{|t| \leq C \|\gamma\|} |\eta(t)| \right) \|g_i - T_n^\top \tilde{g}_i\|.$$

The proof is complete. \square

The next lemma bounds the difference between the sample information matrix \tilde{F} and its population counterpart F , defined in (17) and (13), respectively. This bound will be applied multiple times in the proof of Theorem 1.

Lemma 5 (Information matrix bounds). *Denote $\varphi = (h')^2/v$. Under Assumptions 1, 3, and 5, for sufficiently large n we have*

$$\|T_n^\top \tilde{F}(T_n \gamma) T_n - F(\gamma)\| \leq \Psi(\|\gamma\|) \bar{\tau}_n,$$

where $\Psi : \mathbb{R} \rightarrow \mathbb{R}$ is a non-decreasing function defined by

$$\Psi(s) = C^2 C_2 s \sup_{|t| \leq 2Cs} |\varphi'(t)| + (2C + C_2) C_2 \sup_{|t| \leq 2Cs} |\varphi(t)|.$$

In addition, if Assumption 4 also holds then for any γ such that $\|\gamma - \gamma^*\| < \delta$, we have

$$1/C - \Psi(\|\gamma\|) \bar{\tau}_n \leq \lambda_{\min}(T_n^\top \tilde{F}(T_n \gamma) T_n) \leq \lambda_{\max}(T_n^\top \tilde{F}(T_n \gamma) T_n) \leq C + \Psi(\|\gamma\|) \bar{\tau}_n. \quad (37)$$

Proof of Lemma 5. We proceed to prove the first inequality in Lemma 5. Recall the formulas for \tilde{F} and F in (17) and (13), respectively. Since $\varphi = (h')^2/v$, it follows that

$$\begin{aligned} F(\gamma) &= n^{-1} \sum_{i=1}^n \varphi(g_i^\top \gamma) g_i g_i^\top, \\ T_n^\top \tilde{F}(T_n \gamma) T_n &= n^{-1} \sum_{i=1}^n \varphi(\tilde{g}_i^\top T_n \gamma) T_n^\top \tilde{g}_i \tilde{g}_i^\top T_n. \end{aligned}$$

We will bound $u^\top (T_n^\top \tilde{F}(T_n \gamma) T_n - F(\gamma)) u := \Phi_1 + \Phi_2$ for any fixed unit vector u , where

$$\begin{aligned} \Phi_1 &= n^{-1} \sum_{i=1}^n \varphi(\tilde{g}_i^\top T_n \gamma) u^\top (T_n^\top \tilde{g}_i \tilde{g}_i^\top T_n - g_i g_i^\top) u, \\ \Phi_2 &= n^{-1} \sum_{i=1}^n (\varphi(\tilde{g}_i^\top T_n \gamma) - \varphi(g_i^\top \gamma)) u^\top g_i g_i^\top u. \end{aligned}$$

Regarding Φ_1 , by Assumption 1 and Lemma 1, we have

$$\begin{aligned}
|\Phi_1| &\leq n^{-1} \max_{1 \leq i \leq n} \left| \varphi(\tilde{g}_i^\top T_n \gamma) \right| \sum_{i=1}^n \left| u^\top \left(T_n^\top \tilde{g}_i \tilde{g}_i^\top T_n - g_i g_i^\top \right) u \right| \\
&= n^{-1} \max_{1 \leq i \leq n} \left| \varphi(\tilde{g}_i^\top T_n \gamma) \right| \sum_{i=1}^n \left| \left(u^\top T_n^\top \tilde{g}_i \right)^2 - \left(u^\top g_i \right)^2 \right| \\
&= n^{-1} \max_{1 \leq i \leq n} \left| \varphi(\tilde{g}_i^\top T_n \gamma) \right| \sum_{i=1}^n \left| u^\top (T_n^\top \tilde{g}_i + g_i) \right| \left| u^\top (T_n^\top \tilde{g}_i - g_i) \right| \\
&\leq n^{-1} \max_{1 \leq i \leq n} \left| \varphi(\tilde{g}_i^\top T_n \gamma) \right| \sum_{i=1}^n \left\| T_n^\top \tilde{g}_i + g_i \right\| \left\| T_n^\top \tilde{g}_i - g_i \right\| \\
&\leq n^{-1} \max_{1 \leq i \leq n} \left| \varphi(\tilde{g}_i^\top T_n \gamma) \right| \sum_{i=1}^n \left(\left\| T_n^\top \tilde{g}_i - g_i \right\| + 2\|g_i\| \right) \left\| T_n^\top \tilde{g}_i - g_i \right\| \\
&\leq n^{-1} \max_{1 \leq i \leq n} \left| \varphi(\tilde{g}_i^\top T_n \gamma) \right| \sum_{i=1}^n (C_2 \bar{\tau}_n + 2C) \left\| T_n^\top \tilde{g}_i - g_i \right\| \\
&\leq \left((2C + C_2) \max_{1 \leq i \leq n} \left| \varphi(\tilde{g}_i^\top T_n \gamma) \right| \right) n^{-1} \sum_{i=1}^n \left\| T_n^\top \tilde{g}_i - g_i \right\| \\
&\leq \left((2C + C_2) \max_{1 \leq i \leq n} \left| \varphi(\tilde{g}_i^\top T_n \gamma) \right| \right) C_2 \bar{\tau}_n.
\end{aligned}$$

We now bound $|\Phi_2|$. Denote

$$\varphi_i(t) = \varphi(g_i^\top \gamma + t(T_n^\top \tilde{g}_i - g_i)^\top \gamma).$$

By the Mean Value Theorem, there exists $t^* \in [0, 1]$ and $p_i = \tilde{g}_i^\top T_i + t^*(g_i - T_n^\top \tilde{g}_i)$ such that

$$\begin{aligned}
|\Phi_2| &= n^{-1} \left| \sum_{i=1}^n (u^\top g_i)^2 (\varphi_i(1) - \varphi_i(0)) \right| = n^{-1} \left| \sum_{i=1}^n (u^\top g_i)^2 \varphi'_i(t^*) \right| \\
&= n^{-1} \left| \sum_{i=1}^n (u^\top g_i)^2 \varphi'(p_i^\top \gamma) (T_n^\top \tilde{g}_i - g_i)^\top \gamma \right| \\
&\leq n^{-1} \|\gamma\| \max_{1 \leq i \leq n} |\varphi'(p_i^\top \gamma)| \max_{1 \leq i \leq n} \|g_i\|^2 \sum_{i=1}^n \left\| T_n^\top \tilde{g}_i - g_i \right\| \\
&\leq n^{-1} C^2 \|\gamma\| \max_{1 \leq i \leq n} |\varphi'(p_i^\top \gamma)| \sum_{i=1}^n \left\| T_n^\top \tilde{g}_i - g_i \right\| \\
&\leq C^2 C_2 \|\gamma\| \max_{1 \leq i \leq n} |\varphi'(p_i^\top \gamma)| \bar{\tau}_n,
\end{aligned}$$

where the second inequality follows from Assumption 1 and the last inequality follows from Lemma 1. By Assumption 2, Lemma 1, and (36),

$$\|p_i\| \leq (1 - t^*) \|T_n^\top \tilde{g}_i\| + t^* \|g_i\| \leq t^* C + 2(1 - t^*) C \leq 2C,$$

for sufficiently large n .

Putting these inequalities together, we have

$$\begin{aligned} \left\| T_n^\top \tilde{F}(T_n \gamma) T_n - F(\gamma) \right\| &\leq \left(C^3 \|\gamma\| \max_{1 \leq i \leq n} |\varphi'(p_i^\top \gamma)| + 3C^2 \max_{1 \leq i \leq n} |\varphi(\tilde{g}_i^\top T_n \gamma)| \right) \bar{\tau}_n \\ &\leq \left(C^2 C_2 \|\gamma\| \max_{|t| \leq 2C \|\gamma\|} |\varphi'(t)| + (2C + C_2) C_2 \max_{|t| \leq 2C \|\gamma\|} |\varphi(t)| \right) \bar{\tau}_n. \end{aligned}$$

We now prove the second claim in Lemma 5. From Assumption 4 and the first claim of Lemma 5, we have

$$\lambda_{\min}(T_n^\top \tilde{F}(T_n \gamma) T_n) \geq \lambda_{\min}(F(\gamma)) - \|T_n^\top \tilde{F}(T_n \gamma) T_n - F(\gamma)\| \geq 1/C - \Psi(\|\gamma\|) \bar{\tau}_n.$$

Similarly,

$$\lambda_{\max}(T_n^\top \tilde{F}(T_n \gamma) T_n) \leq \lambda_{\max}(F(\gamma)) + \|T_n^\top \tilde{F}(T_n \gamma) T_n - F(\gamma)\| \leq C + \Psi(\|\gamma\|) \bar{\tau}_n.$$

The proof is completed. \square

A direct consequence of (37) with $\gamma = \gamma^*$ is that the scaling matrix $T_n^\top \tilde{F}(T_n \gamma^*) T_n$, which appears in the proof of Theorem 1, is well-conditioned.

Corollary 5 (Scaling matrix is well-conditioned). *Assume that the conditions in Lemma 5 hold. Then, as n is sufficiently large,*

$$\frac{1}{2C} \leq \lambda_{\min}(T_n^\top \tilde{F}(T_n \gamma^*) T_n) \leq \lambda_{\max}(T_n^\top \tilde{F}(T_n \gamma^*) T_n) \leq 2C. \quad (38)$$

Proof of Corollary 5. Let Ψ be the function defined in Lemma 5. By Remarks 1 and 2, we have

$$\Psi(\|\gamma^*\|) = C^2 C_2 \|\gamma^*\| \sup_{|t| \leq 2C \|\gamma^*\|} |\varphi'(t)| + 3CC_2 \sup_{|t| \leq 2C \|\gamma^*\|} |\varphi(t)| \leq 3C^3 C_2 M + 3CC_2 M.$$

Since it is assumed that $\bar{\tau}_n \rightarrow 0$, this implies $\Psi(\|\gamma^*\|) \bar{\tau}_n$ is close to zero as n is sufficiently large, and (37) implies (38). \square

The following lemma shows that the estimating equation (12) and its sample counterpart (16) are sufficiently close.

Lemma 6 (Estimating equation bounds). *Under the Assumption 1, 3, 5 and 6, we have*

$$\left\| T_n^\top \tilde{S}(T_n \gamma^*) - S(\gamma^*) \right\| = o_p(n^{-1/2}) \quad (39)$$

and

$$\left\| \mathbb{E} \left(T_n^\top \tilde{S}(T_n \gamma^*) - S(\gamma^*) \right) \right\| = o(n^{-1/2}). \quad (40)$$

We need the following lemma to prove Lemma 6.

Lemma 7 (Lemma 5.1 in Stefanski and Carroll [1985]). *Let $(U_i)_{i=1}^\infty$ be a sequence of independent random variables with zero means and $\mathbb{E}[|U_i|^{1+\zeta}] < \infty$ for all i and some $\zeta > 0$. If a sequence of scalars $(a_i)_{i=1}^\infty$ satisfies $\sum_{i=1}^n |a_i| = O(n)$ and $\max_{1 \leq i \leq n} |a_i| = o(n)$ then $\sum_{i=1}^n a_i U_i = o_p(n)$.*

Proof of Lemma 6. For the notation convenience, denote $\eta = h'/v : \mathbb{R} \rightarrow \mathbb{R}$. Then,

$$\begin{aligned} S(\gamma^*) &= \frac{1}{n} \sum_{i=1}^n g_i \eta \left(g_i^\top \gamma^* \right) \left[y_i - h \left(g_i^\top \gamma^* \right) \right], \\ T_n^\top \tilde{S}(T_n \gamma^*) &= \frac{1}{n} \sum_{i=1}^n T_n^\top \tilde{g}_i \eta \left(\tilde{g}_i^\top T_n \gamma^* \right) \left[y_i - h \left(\tilde{g}_i^\top T_n \gamma^* \right) \right]. \end{aligned}$$

We first bound the difference between their expectations:

$$\mathbb{E} \left[T_n^\top \tilde{S}(T_n \gamma^*) - S(\gamma^*) \right] =: B_1 - B_2,$$

where

$$\begin{aligned} B_1 &= \frac{1}{n} \sum_{i=1}^n \left[T_n^\top \tilde{g}_i \eta (\tilde{g}_i^\top T_n \gamma^*) - g_i \eta (g_i^\top \gamma^*) \right] h(g_i^\top \gamma^*), \\ B_2 &= \frac{1}{n} \sum_{i=1}^n \left[T_n^\top \tilde{g}_i \eta (\tilde{g}_i^\top T_n \gamma^*) h(\tilde{g}_i^\top T_n \gamma^*) - g_i \eta (g_i^\top \gamma^*) h(g_i^\top \gamma^*) \right]. \end{aligned}$$

By the triangle inequality, Lemma 4 and covariate bound (28) we have in Lemma 1,

$$\begin{aligned} \|B_1\| &\leq n^{-1} \max_{1 \leq i \leq n} |h(g_i^\top \gamma^*)| \sum_{i=1}^n \left\| \left(T_n^\top \tilde{g}_i \eta (\tilde{g}_i^\top T_n \gamma^*) - g_i \eta (g_i^\top \gamma^*) \right) \right\| \\ &\leq n^{-1} \sup_{|t| \leq C \|\gamma^*\|} |h(t)| \left(2C \|\gamma^*\| \sup_{|t| \leq 2C \|\gamma^*\|} |\eta'(t)| + \sup_{|t| \leq C \|\gamma^*\|} |\eta(t)| \right) \sum_{i=1}^n \|T_n^\top \tilde{g}_i - g_i\| \\ &\leq C_2 \bar{\tau}_n \sup_{|t| \leq C \|\gamma^*\|} |h(t)| \left(2C \|\gamma^*\| \sup_{|t| \leq 2C \|\gamma^*\|} |\eta'(t)| + \sup_{|t| \leq C \|\gamma^*\|} |\eta(t)| \right). \end{aligned}$$

Then by the bound for $\|\gamma^*\|$ and for the continuous function in Remarks 1 and 2,

$$\|B_1\| \leq C_2 (6C^2 + 1) M^2 \bar{\tau}_n = o(n^{-1/2}). \quad (41)$$

Similarly, for B_2 we have

$$\begin{aligned} \|B_2\| &\leq n^{-1} \sum_{i=1}^n \left\| \left(T_n^\top \tilde{g}_i (\eta \cdot h) (\tilde{g}_i^\top T_n \gamma^*) - g_i (\eta \cdot h) (g_i^\top \gamma^*) \right) \right\| \\ &\leq n^{-1} \left(2C \|\gamma^*\| \sup_{|t| \leq 2C \|\gamma^*\|} |(\eta \cdot h)'(t)| + \sup_{|t| \leq C \|\gamma^*\|} |(\eta \cdot h)(t)| \right) \sum_{i=1}^n \|T_n^\top \tilde{g}_i - g_i\| \\ &\leq C_2 \bar{\tau}_n \left(2C \|\gamma^*\| \sup_{|t| \leq 2C \|\gamma^*\|} |(\eta \cdot h)'(t)| + \sup_{|t| \leq C \|\gamma^*\|} |(\eta \cdot h)(t)| \right) \\ &\leq C_2 (6C^2 + 1) M \bar{\tau}_n = o(n^{-1/2}). \end{aligned} \quad (42)$$

By (41), (42), we have (40).

Next, we prove the convergence in probability for the random part:

$$T_n^\top \tilde{S}(T_n \gamma^*) - S(\gamma^*) - \mathbb{E} \left(T_n^\top \tilde{S}(T_n \gamma^*) - S(\gamma^*) \right) = n^{-1} \sum_{i=1}^n \left(T_n^\top \tilde{g}_i \eta \left(\tilde{g}_i^\top T_n \gamma^* \right) - g_i \eta \left(g_i^\top \gamma^* \right) \right) e_i,$$

The j th element of it is

$$\left(n^{-1} \sum_{i=1}^n \left(T_n^\top \tilde{g}_i \eta \left(\tilde{g}_i^\top T_n \gamma^* \right) - g_i \eta \left(g_i^\top \gamma^* \right) \right) e_i \right)_j := n^{-1} \sum_{i=1}^n \left(T_n^\top \tilde{g}_i \eta \left(\tilde{g}_i^\top T_n \gamma^* \right) - g_i \eta \left(g_i^\top \gamma^* \right) \right)_j e_i.$$

We will apply Lemma 7 to the right-hand side of the above equation with

$$U_i = e_i, \quad a_i = n^{1/2} (T_n^\top \tilde{g}_i \eta \left(\tilde{g}_i^\top T_n \gamma^* \right) - g_i \eta \left(g_i^\top \gamma^* \right))_j.$$

To this end, we need to verify the three conditions in Lemma 7. Condition $\mathbb{E}[|U_i|^{1+\zeta}] < \infty$ holds with $\xi = 1$ due to Lemma 1:

$$\mathbb{E}[|U_i|^2] = \mathbb{E}[e_i^2] = v(g_i^\top \gamma^*) \leq \sup_{|t| \leq C \|\gamma^*\|} v(t) \leq M.$$

Condition $\max_{1 \leq i \leq n} |a_i| = o(n)$ holds because

$$\begin{aligned} n^{-1/2} \max_{1 \leq i \leq n} |a_i| &\leq \max_{1 \leq i \leq n} \left\| T_n^\top \tilde{g}_i \eta \left(\tilde{g}_i^\top T_n \gamma^* \right) \right\| + \max_{1 \leq i \leq n} \left\| g_i \eta \left(g_i^\top \gamma^* \right) \right\| \\ &\leq \max_{1 \leq i \leq n} \left\| T_n^\top \tilde{g}_i \right\| \max_{1 \leq i \leq n} \left| \eta \left(\tilde{g}_i^\top T_n \gamma^* \right) \right| + \max_{1 \leq i \leq n} \|g_i\| \max_{1 \leq i \leq n} \left| \eta \left(g_i^\top \gamma^* \right) \right| \\ &\leq 2C \max_{|t| \leq 2C \|\gamma^*\|} |\eta(t)| + C \max_{|t| \leq C \|\gamma^*\|} |\eta(t)| \\ &\leq 3CM. \end{aligned}$$

Finally, condition $\sum_{i=1}^n |a_i| = O(n)$ holds due to Lemma 4:

$$\begin{aligned} \sum_{i=1}^n |a_i| &\leq n^{1/2} C_2 \bar{\tau}_n \left(2C \|\gamma^*\| \sup_{|t| \leq n^{3/2} 2C \|\gamma^*\|} |\eta'(t)| + \sup_{|t| \leq C \|\gamma^*\|} |\eta(t)| \right) \\ &\leq n^{3/2} C_2 (6C^2 + 1) M \bar{\tau}_n = o(n). \end{aligned}$$

Therefore, by Lemma 7, we have

$$n^{-1} \sum_{i=1}^n \left(T_n^\top \tilde{g}_i \eta \left(\tilde{g}_i^\top T_n \gamma^* \right) - g_i \eta \left(g_i^\top \gamma^* \right) \right)_j e_i = o_p(n^{-1/2}),$$

which implies that

$$\left\| T_n^\top \tilde{S}(T_n \gamma^*) - S(\gamma^*) - \mathbb{E} \left(T_n^\top \tilde{S}(T_n \gamma^*) - S(\gamma^*) \right) \right\| = o_p(n^{-1/2}). \quad (43)$$

By (43) and (40),

$$\begin{aligned}
\left\| T_n^\top \tilde{S}(T_n \gamma^*) - S(\gamma^*) \right\| &\leq \left\| T_n^\top \tilde{S}(T_n \gamma^*) - S(\gamma^*) - \mathbb{E} \left(T_n^\top \tilde{S}(T_n \gamma^*) - S(\gamma^*) \right) \right\| \\
&\quad + \left\| \mathbb{E} \left(T_n^\top \tilde{S}(T_n \gamma^*) - S(\gamma^*) \right) \right\| \\
&= o_p(n^{-1/2}) + o(n^{-1/2}) \\
&= o_p(n^{-1/2}).
\end{aligned}$$

The proof is completed. \square

Lemma 8 (Bound on the gradient of the score function). *Under Assumptions 1 to 5,*

$$\sup_{\gamma \in N_n(\delta_0)} \left\| T_n^\top (\partial \tilde{S}(\gamma) / \partial \gamma^\top) T_n - T_n^\top \tilde{F}(T_n \gamma^*) T_n \right\| = o(1),$$

where

$$N_n(\delta_0) := \left\{ \gamma : \|T_n^{-1} \gamma - \gamma^*\| \leq (2C/n)^{1/2} \delta_0 \right\}.$$

Proof of Lemma 8. Using the definition of \tilde{S} in (16), we rewrite $T_n^\top (\partial \tilde{S}(\gamma) / \partial \gamma^\top) T_n$ as follows:

$$T_n^\top (\partial \tilde{S}(\gamma) / \partial \gamma^\top) T_n = -T_n^\top \tilde{F}(\gamma) T_n + \frac{1}{n} \sum_{i=1}^n \eta'(\tilde{g}_i^\top \gamma) \left(y_i - h(\tilde{g}_i^\top \gamma) \right) T_n^\top \tilde{g}_i \tilde{g}_i^\top T_n, \quad (44)$$

where $\eta = h'/v$ is a scalar function depending on functions h and v in the definition of \tilde{S} . We will show that the first term on the right-hand side of (44) is close to its population counterpart $T_n^\top \tilde{F}(T_n \gamma^*) T_n$ while the second term is negligible.

We proceed to prove the first part of the claim above. According to (17), we have

$$\tilde{F}(\gamma) = \frac{1}{n} \sum_{i=1}^n (\eta \cdot h')(\tilde{g}_i^\top \gamma) \tilde{g}_i \tilde{g}_i^\top.$$

Therefore,

$$\begin{aligned}
T_n^\top \tilde{F}(\gamma) T_n - T_n^\top \tilde{F}(T_n \gamma^*) T_n &= \frac{1}{n} \sum_{i=1}^n \left[(\eta \cdot h')(\tilde{g}_i^\top \gamma) - (\eta \cdot h')(\tilde{g}_i^\top T_n \gamma^*) \right] T_n^\top \tilde{g}_i \tilde{g}_i^\top T_n \\
&= \frac{1}{n} \sum_{i=1}^n [\varphi_i(1) - \varphi_i(0)] T_n^\top \tilde{g}_i \tilde{g}_i^\top T_n,
\end{aligned}$$

where

$$\varphi_i(t) := (\eta \cdot h') \left(t \tilde{g}_i^\top \gamma + (1-t) \tilde{g}_i^\top T_n \gamma^* \right).$$

By the Mean Value Theorem, there exist $t_i \in [0, 1]$ and $\bar{\gamma}_i = t_i \gamma + (1-t_i) T_n \gamma^*$ such that

$$\varphi_i(1) - \varphi_i(0) = \varphi_i'(t_i) = \tilde{g}_i^\top (\gamma - T_n \gamma^*) (\eta \cdot h')' \left(\tilde{g}_i^\top \bar{\gamma}_i \right).$$

Substituting this into the equation above, we get

$$T_n^\top \tilde{F}(\gamma) T_n - T_n^\top \tilde{F}(T_n \gamma^*) T_n = \frac{1}{n} \sum_{i=1}^n \tilde{g}_i^\top (\gamma - T_n \gamma^*) (\eta \cdot h')' (\tilde{g}_i^\top \tilde{\gamma}_i) T_n^\top \tilde{g}_i \tilde{g}_i^\top T_n.$$

We now bound the terms on the right-hand side. First, by (27) and the definition of $N_n(\delta_0)$, we have

$$\left| \tilde{g}_i^\top (\gamma - T_n \gamma^*) \right| \leq \left\| \tilde{g}_i^\top T_n \right\| \left\| T_n^{-1} (\gamma - T_n \gamma^*) \right\| \leq 2C \left\| T_n^{-1} \gamma - \gamma^* \right\| = O(n^{-1/2}).$$

Next, by (35) and (36),

$$\begin{aligned} \left| \tilde{g}_i^\top \tilde{\gamma}_i \right| &\leq \left\| \tilde{g}_i^\top T_n \right\| \cdot \left\| T_n^{-1} \tilde{\gamma}_i \right\| = \left\| T_n^\top \tilde{g}_n \right\| \cdot \left\| t_i T_n^{-1} \gamma + (1 - t_i) \gamma^* \right\| \\ &\leq 2C (t_i \left\| T_n^{-1} \gamma \right\| + (1 - t_i) \left\| \gamma^* \right\|). \end{aligned}$$

Since $\gamma \in N_n(\delta_0)$, it follows that for sufficiently large n ,

$$\left\| T_n^{-1} \gamma \right\| \leq \left\| T_n^{-1} \gamma - \gamma^* \right\| + \left\| \gamma^* \right\| \leq (2C/n)^{1/2} \delta_0 + \left\| \gamma^* \right\| \leq 2 \left\| \gamma^* \right\|. \quad (45)$$

Therefore, the last two bounds imply $|\tilde{g}_i^\top \tilde{\gamma}_i| \leq 4C \left\| \gamma^* \right\|$. Since $(\eta \cdot h')'$ is a smooth function, we obtain that $|(\eta \cdot h')'(\tilde{g}_i^\top \tilde{\gamma}_i)|$ is uniformly bounded over $1 \leq i \leq n$ and $\gamma \in N_n(\delta_0)$. Finally, by (36) and for sufficiently large n , we have

$$\left\| T_n^\top \tilde{g}_i \tilde{g}_i^\top T_n \right\| = \left\| T_n^\top \tilde{g}_i \right\|^2 \leq 4C^2. \quad (46)$$

Putting these inequalities together, we obtain

$$\max_{\gamma \in N_n(\delta_0)} \left\| T_n^\top \tilde{F}(\gamma) T_n - T_n^\top \tilde{F}(T_n \gamma^*) T_n \right\| = O(n^{-1/2}).$$

We now show that the second term on the right-hand side of (44) is negligible. To this end, we decompose it as $\Phi_1 - \Phi_2 - \Phi_3$, where

$$\begin{aligned} \Phi_1 &= \frac{1}{n} \sum_{i=1}^n \eta' \left(\tilde{g}_i^\top \gamma \right) \left(h \left(\tilde{g}_i^\top \gamma \right) - h \left(\tilde{g}_i^\top \gamma^* \right) \right) T_n^\top \tilde{g}_i \tilde{g}_i^\top T_n, \\ \Phi_2 &= \frac{1}{n} \sum_{i=1}^n \eta' \left(\tilde{g}_i^\top T_n \gamma^* \right) e_i T_n^\top \tilde{g}_i \tilde{g}_i^\top T_n, \\ \Phi_3 &= \frac{1}{n} \sum_{i=1}^n \left(\eta' \left(\tilde{g}_i^\top \gamma \right) - \eta' \left(\tilde{g}_i^\top T_n \gamma^* \right) \right) e_i T_n^\top \tilde{g}_i \tilde{g}_i^\top T_n. \end{aligned}$$

Note that Φ_1 is the expectation of the second term on the right-hand side of (44), while $-\Phi_2 - \Phi_3$ is its centered version, where Φ_2 does not depend on γ and Φ_3 depends on γ . We will bound $\Phi_1, \Phi_2,$

and Φ_3 separately. Regarding Φ_1 , by (46) and the triangle inequality,

$$\begin{aligned}\|\Phi_1\| &\leq \frac{1}{n} \sum_{i=1}^n \left| \eta'(\tilde{g}_i^\top \gamma) \right| \left| h(\tilde{g}_i^\top \gamma) - h(g_i^\top \gamma^*) \right| \|T_n^\top \tilde{g}_i \tilde{g}_i^\top T_n\| \\ &\leq \frac{4C^2}{n} \sum_{i=1}^n \left| \eta'(\tilde{g}_i^\top \gamma) \right| \left| h(\tilde{g}_i^\top \gamma) - h(g_i^\top \gamma^*) \right| \\ &\leq \frac{4C^2}{n} \sum_{i=1}^n \left| \eta'(\tilde{g}_i^\top \gamma) \right| \left\{ \left| h(\tilde{g}_i^\top \gamma) - h(g_i^\top T_n^{-1} \gamma) \right| + \left| h(g_i^\top T_n^{-1} \gamma) - h(g_i^\top \gamma^*) \right| \right\}.\end{aligned}$$

We now bound the terms on the right-hand side of the inequality above. By the Mean Value Theorem, there exists $\tilde{t}_i \in [0, 1]$ and $\tilde{\gamma}_i = \tilde{t}_i T_n^{-1} \gamma + (1 - \tilde{t}_i) \gamma^*$ such that

$$\left| h(g_i^\top T_n^{-1} \gamma) - h(g_i^\top \gamma^*) \right| = \left| h'(g_i^\top \tilde{\gamma}_i) g_i^\top (T_n^{-1} \gamma - \gamma^*) \right| \leq \left| h'(g_i^\top \tilde{\gamma}_i) \right| \|g_i\| \|T_n^{-1} \gamma - \gamma^*\|.$$

By Assumption 3, (45), and (27), we have

$$\begin{aligned}\left| g_i^\top \tilde{\gamma}_i \right| &\leq \tilde{t}_i \left| g_i^\top T_n^{-1} \gamma \right| + (1 - \tilde{t}_i) \left| g_i^\top \gamma^* \right| \leq \tilde{t}_i \|g_i\| \|T_n^{-1} \gamma\| + (1 - \tilde{t}_i) \|g_i\| \|\gamma^*\| \\ &\leq 2\tilde{t}_i C \|\gamma^*\| + (1 - \tilde{t}_i) C \|\gamma^*\| \\ &\leq 2C \|\gamma^*\|.\end{aligned}$$

Since h' is a smooth function, this implies that $|h'(g_i^\top \tilde{\gamma}_i)|$ is uniformly bounded over $1 \leq i \leq n$. Moreover, $\|g_i\| \leq C$ by Assumption 3 and $\|T_n^{-1} \gamma - \gamma^*\| \leq (2C/n)^{1/2} \delta_0$ because $\gamma \in N_n(\delta_0)$. Therefore,

$$\left| h(g_i^\top T_n^{-1} \gamma) - h(g_i^\top \gamma^*) \right| = O(n^{-1/2}).$$

Similarly, there exist $\bar{t}_i \in [0, 1]$ and $\bar{g}_i = \bar{t}_i T_n^\top \tilde{g}_i + (1 - \bar{t}_i) g_i$ such that

$$\begin{aligned}\left| h(\tilde{g}_i^\top \gamma) - h(g_i^\top T_n^{-1} \gamma) \right| &= \left| h'(\bar{g}_i^\top T_n^{-1} \gamma) (\tilde{g}_i^\top T_n - g_i^\top) T_n^{-1} \gamma \right| \\ &\leq \left| h'(\bar{g}_i^\top T_n^{-1} \gamma) \right| \left\| T_n^\top \tilde{g}_i - g_i \right\| \|T_n^{-1} \gamma\|.\end{aligned}$$

By (27), Assumption 5, and (45),

$$\left\| T_n^\top \tilde{g}_i - g_i \right\| \leq C_2 n^{1/2} \bar{\tau}_n = o(1), \quad \|T_n^{-1} \gamma\| \leq 2 \|\gamma^*\|.$$

Again, by (27), for sufficiently large n ,

$$\|\bar{g}_i\| = \left\| g_i + \bar{t}_i (T_n^\top \tilde{g}_i - g_i) \right\| \leq \|g_i\| + \bar{t}_i \left\| T_n^\top \tilde{g}_i - g_i \right\| \leq C + \bar{t}_i C_2 n^{1/2} \bar{\tau}_n \leq 2C.$$

Since h' is a smooth function, we obtain

$$\left| h(\tilde{g}_i^\top \gamma) - h(g_i^\top T_n^{-1} \gamma) \right| = o(1).$$

Finally, by (45) and (46),

$$|\tilde{g}_i^\top \gamma| \leq \|T_n^\top \tilde{g}_i\| \cdot \|T_n^{-1} \gamma\| \leq 4C \|\gamma^*\|,$$

which, together with the smoothness of η' , implies that $|\eta'(\tilde{g}_i^\top \gamma)|$ is uniformly bounded over $1 \leq i \leq n$ and $\gamma \in N_n(\delta_0)$. Putting these inequalities together, we obtain $\|\Phi_1\| = o(1)$.

Next, we show that Φ_2 is negligible by bounding its entries (Φ_2 is a matrix with a bounded number of entries). For $1 \leq s, t \leq p + K - r$, we have

$$(\Phi_2)_{st} = \frac{1}{n} \sum_{i=1}^n \eta'(\tilde{g}_i^\top T_n \gamma^*) \left(T_n^\top \tilde{g}_i \tilde{g}_i^\top T_n \right)_{st} e_i.$$

By (46), we have

$$\left| \left(T_n^\top \tilde{g}_i \tilde{g}_i^\top T_n \right)_{st} \right| \leq 4C^2, \quad \left| \tilde{g}_i^\top T_n \gamma^* \right| \leq \left\| T_n^\top \tilde{g}_i \right\| \|\gamma^*\| \leq 2C \|\gamma^*\|.$$

Since η' is a continuous function, it follows that the coefficients $\eta'(\tilde{g}_i^\top T_n \gamma^*) \left(T_n^\top \tilde{g}_i \tilde{g}_i^\top T_n \right)_{st}$ in the formula for $(\Phi_2)_{st}$ are uniformly bounded over $1 \leq i \leq n$. Note also that e_i , $1 \leq i \leq n$, are independent mean-zero random variables with variances $v(g_i^\top \gamma^*)$. These variances are uniformly bounded over $1 \leq i \leq n$ because $|g_i^\top \gamma^*| \leq \|g_i\| \|\gamma^*\| \leq C \|\gamma^*\|$ by Assumption 3 and v is a smooth function. Therefore, by Markov inequality, for any $t > 0$,

$$\mathbb{P}((\Phi_2)_{st} \geq t) \leq (tn)^{-2} \sum_{i=1}^n \left(\eta'(\tilde{g}_i^\top T_n \gamma^*) \right)^2 \left(\left(T_n^\top \tilde{g}_i \tilde{g}_i^\top T_n \right)_{st} \right)^2 v(g_i^\top \gamma^*) = O(t^{-2} n^{-1}).$$

Choosing $t = o(n^{-1/2})$, we obtain $\|\Phi_2\| = o_p(1)$.

Finally, we bound Φ_3 . By the Mean Value Theorem, there exists $\tilde{t}_i \in [0, 1]$ and $\check{\gamma}_i = \tilde{t}_i T_n^{-1} \gamma + (1 - \tilde{t}_i) \gamma^*$ such that

$$\eta'(\tilde{g}_i^\top \gamma) - \eta'(\tilde{g}_i^\top T_n \gamma^*) = \eta''(\tilde{g}_i^\top T_n \check{\gamma}_i) \tilde{g}_i^\top T_n (T_n^{-1} \gamma - \gamma^*).$$

By (45) and (46),

$$\begin{aligned} \left| \tilde{g}_i^\top T_n \check{\gamma}_i \right| &\leq \tilde{t}_i \left| \tilde{g}_i^\top \gamma \right| + (1 - \tilde{t}_i) \left| \tilde{g}_i^\top T_n \gamma^* \right| \\ &\leq \tilde{t}_i \left\| T_n^\top \tilde{g}_i \right\| \|\gamma\| + (1 - \tilde{t}_i) \left\| T_n^\top \tilde{g}_i \right\| \|\gamma^*\| \\ &\leq 4\tilde{t}_i C \|\gamma^*\| + 2(1 - \tilde{t}_i) C \|\gamma^*\| \\ &\leq 4C \|\gamma^*\|. \end{aligned}$$

Since η'' is a smooth function, this implies that $\eta''(\tilde{g}_i^\top T_n \check{\gamma}_i)$ is uniformly bounded over $1 \leq i \leq n$ and $\gamma \in N_n(\delta_0)$ by a constant $M > 0$. Therefore by (46) and the definition of $N_n(\delta_0)$,

$$\begin{aligned} \|\Phi_3\| &= \left\| \frac{1}{n} \sum_{i=1}^n \eta''(\tilde{g}_i^\top T_n \check{\gamma}_i) \tilde{g}_i^\top T_n (T_n^{-1} \gamma - \gamma^*) e_i T_n^\top \tilde{g}_i \tilde{g}_i^\top T_n \right\| \\ &\leq \frac{8C^3 M}{n} \sum_{i=1}^n \|T_n^{-1} \gamma - \gamma^*\| |e_i| \\ &\leq (8C^3 M)(2C/n)^{1/2} \delta_0 \left(\frac{1}{n} \sum_{i=1}^n |e_i| \right). \end{aligned}$$

Since the variances of e_i are uniformly bounded over $1 \leq i \leq n$ (see the argument for Φ_2 above), it follows that

$$\begin{aligned} \mathbb{E} \left[\sup_{\gamma \in N_n(\delta_0)} \|\Phi_3\| \right] &\leq O(n^{-1/2}) \cdot \mathbb{E} \left[\frac{1}{n} \sum_{i=1}^n |e_i| \right] \leq O(n^{-1/2}) \cdot \max_{1 \leq i \leq n} \mathbb{E} |e_i| \\ &\leq O(n^{-1/2}) \cdot \max_{1 \leq i \leq n} \sqrt{\mathbb{E} |e_i|^2} \rightarrow 0. \end{aligned}$$

In turns, this implies $\sup_{\gamma \in N_n(\delta_0)} \|\Phi_3\| = o_p(1)$ by the Markov inequality. The proof is complete. \square

We also need the following lemma for the proof of Lemma 3.

Lemma 9 (Lemma 2 in [Yin et al. \[2006\]](#)). *Let $f : G \subset \mathbb{R}^q \rightarrow \mathbb{R}^q$ be a function with $f(x) = (f_1(x), \dots, f_q(x))^\top$ such that f_1, \dots, f_q are continuously differentiable on the convex set G . Then for any $\alpha, \beta \in G$,*

$$f(\beta) - f(\alpha) = \left(\int_0^1 \frac{\partial f(\alpha + t(\beta - \alpha))}{\partial x} dt \right) (\beta - \alpha),$$

where the integral is taken element-wise.

Proof of Lemma 3. We first prove (33). By Lemma 9,

$$T_n^\top \tilde{S}(\gamma) - T_n^\top \tilde{S}(T_n \gamma^*) = \mathbb{H}(\gamma)(T_n^{-1} \gamma - \gamma^*), \quad (47)$$

where for notation simplicity, we denote

$$\mathbb{H}(\gamma) = \int_0^1 H(\gamma^* + t(T_n^{-1} \gamma - \gamma^*)) dt, \quad H(\gamma) = T_n^\top (\partial \tilde{S}(\gamma) / \partial \gamma^\top) T_n.$$

We show that $\mathbb{H}(\gamma)$ is well-conditioned. For that purpose, we decompose $\mathbb{H} = \Phi_1 + \Phi_2$, where $\Phi_1 = T_n^\top \tilde{F}(T_n \gamma^*) T_n$ and $\Phi_2 = \mathbb{H}(\gamma) - \Phi_1$. From Corollary 5,

$$\lambda_{\min}(\Phi_1) = \lambda_{\min} \left(T_n^\top \tilde{F}(T_n \gamma^*) T_n \right) \geq \frac{1}{2C}.$$

Regarding Φ_2 , by Lemma 8,

$$\begin{aligned} \|\Phi_2\| &= \left\| \int_0^1 \left[H(\gamma^* + t(T_n^{-1} \gamma - \gamma^*)) - T_n^\top \tilde{F}(T_n \gamma^*) T_n \right] dt \right\| \\ &\leq \int_0^1 \left\| H(\gamma^* + t(T_n^{-1} \gamma - \gamma^*)) - T_n^\top \tilde{F}(T_n \gamma^*) T_n \right\| dt \\ &= o_p(1). \end{aligned} \quad (48)$$

For any $\gamma \in \partial N_n(\delta_0)$ we have $\|T_n^{-1} \gamma - \gamma^*\| = \delta_0 n^{-1/2}$. Therefore, by (47),

$$\left\| T_n^\top \tilde{S}(\gamma) - T_n^\top \tilde{S}(T_n \gamma^*) \right\| \geq \lambda_{\min}(\mathbb{H}(\gamma)) \delta_0 n^{-1/2} \geq \left(\frac{1}{2C} + o_p(1) \right) \delta_0 n^{-1/2},$$

and (33) is proved.

We now prove (34). By the triangle inequality,

$$\left\| T_n^\top \tilde{S}(T_n \gamma^*) \right\| \leq \|S(\gamma^*)\| + \left\| T_n^\top \tilde{S}(T_n \gamma^*) - S(\gamma^*) \right\|.$$

The second term on the right-hand side of the above inequality is negligible because by (39),

$$\left\| T_n^\top \tilde{S}(T_n \gamma^*) - S(\gamma^*) \right\| = o_p(n^{-1/2}).$$

It remains to bound $\|S(\gamma^*)\|$. Note that it follows directly from the definition of $S(\gamma^*)$ in (12) that $\mathbb{E}[S(\gamma^*)] = 0$ and $\text{Cov}(S(\gamma^*)) = n^{-1}F(\gamma^*)$ is a square matrix of size $(p + K - r)$. Therefore, by Markov inequality and Assumption 4, for any $t > 0$,

$$\begin{aligned} \mathbb{P}(\|S(\gamma^*)\| > t) &\leq t^{-2} \mathbb{E} \|S(\gamma^*)\|^2 = t^{-2} \mathbb{E} \left[\text{Trace} \left(S^\top(\gamma^*) S(\gamma^*) \right) \right] \\ &= t^{-2} \mathbb{E} \left[\text{Trace} \left(S(\gamma^*) S^\top(\gamma^*) \right) \right] = t^{-2} \text{Trace} \left(\mathbb{E} \left[S(\gamma^*) S^\top(\gamma^*) \right] \right) \\ &= t^{-2} n^{-1} \text{Trace} (F(\gamma^*)) \leq t^{-2} n^{-1} (p + K - r) C. \end{aligned}$$

Choosing $t = O((\varepsilon n)^{-1/2})$, we obtain $\|S(\gamma^*)\| = O(n^{-1/2})$ with probability at least $1 - \varepsilon$. The proof is complete. \square

E The Proof of Theorem 3

We prove Theorem 3 in this section. We will use the notations and results in the proof of Theorem 1. The following lemma is crucial for proving Theorem 3.

Lemma 10 (Asymptotic Approximation). *Assume that the conditions of Theorem 3 hold. Then*

$$T_n^{-1} \hat{\gamma} - \gamma^* = F^{-1}(\gamma^*) S(\gamma^*) + o_p(n^{-1/2}).$$

Proof of Lemma 10. From (47) and the fact that $\hat{\gamma}$ is a solution of the estimating equation, we have

$$0 = T_n^\top \tilde{S}(\hat{\gamma}) = \mathbb{H}(\hat{\gamma})(T_n^{-1} \hat{\gamma} - \gamma^*) + T_n^\top \tilde{S}(T_n \gamma^*),$$

where we recall that

$$\mathbb{H}(\gamma) = \int_0^1 H(\gamma^* + t(T_n^{-1} \gamma - \gamma^*)) dt, \quad H(\gamma) = T_n^\top (\partial \tilde{S}(\gamma) / \partial \gamma^\top) T_n.$$

From the equality above,

$$T_n^{-1} \hat{\gamma} - \gamma^* = \mathbb{H}^{-1}(\hat{\gamma}) T_n^\top \tilde{S}(T_n \gamma^*).$$

In light of Lemma 8 and particularly the bound (48) in its proof, we will approximate $\mathbb{H}(\hat{\gamma})$ by $T_n^\top \tilde{F}(T_n \gamma^*) T_n$, and in turn by $F(\gamma^*) T_n$. Accordingly, we decompose the expression above as

$$\begin{aligned} T_n^{-1} \hat{\gamma} - \gamma^* &= \left(T_n^\top \tilde{F}(T_n \gamma^*) T_n \right)^{-1} T_n^\top \tilde{S}(T_n \gamma^*) + \Phi_1 \\ &= F^{-1}(\gamma^*) S(\gamma^*) + \Phi_2 + \Phi_1, \end{aligned}$$

where Φ_1 and Φ_2 are the errors of those approximations, namely,

$$\begin{aligned}\Phi_1 &= \left[\mathbb{H}^{-1}(\hat{\gamma}) - \left(T_n^\top \tilde{F}(T_n \gamma^*) T_n \right)^{-1} \right] T_n^\top \tilde{S}(T_n \gamma^*), \\ \Phi_2 &= \left(T_n^\top \tilde{F}(T_n \gamma^*) T_n \right)^{-1} T_n^\top \tilde{S}(T_n \gamma^*) - F^{-1}(\gamma^*) S(\gamma^*).\end{aligned}$$

We proceed to bound Φ_1 and then Φ_2 . By (34), we have $\|T_n^\top \tilde{S}(T_n \gamma^*)\| = O_p(n^{-1/2})$. In addition, by Corollary 5, all eigenvalues of $T_n^\top \tilde{F}(T_n \gamma^*) T_n$ belong to interval $[1/(2C), 2C]$, and therefore are bounded away from zero and infinity. Moreover, by (48),

$$\left\| \mathbb{H}(\hat{\gamma}) - T_n^\top \tilde{F}(T_n \gamma^*) T_n \right\| = o_p(1).$$

These imply, in particular, that $\|\mathbb{H}^{-1}(\hat{\gamma})\|$ and $\|(T_n^\top \tilde{F}(T_n \gamma^*) T_n)^{-1}\|$ are both bounded by some constant due to the continuity of the inverse map away from zero. Therefore,

$$\begin{aligned}\|\Phi_1\| &= \left\| \mathbb{H}^{-1}(\hat{\gamma}) \left[\mathbb{H}(\hat{\gamma}) - T_n^\top \tilde{F}(T_n \gamma^*) T_n \right] \left(T_n^\top \tilde{F}(T_n \gamma^*) T_n \right)^{-1} T_n^\top \tilde{S}(T_n \gamma^*) \right\| \\ &\leq \|\mathbb{H}^{-1}(\hat{\gamma})\| \left\| \mathbb{H}(\hat{\gamma}) - T_n^\top \tilde{F}(T_n \gamma^*) T_n \right\| \left\| \left(T_n^\top \tilde{F}(T_n \gamma^*) T_n \right)^{-1} \right\| \left\| T_n^\top \tilde{S}(T_n \gamma^*) \right\| \\ &= o_p(n^{-1/2}).\end{aligned}$$

Next, we bound Φ_2 . By adding and subtracting $(T_n^\top \tilde{F}(T_n \gamma^*) T_n)^{-1} S(\gamma^*)$ and using the triangle inequality, we obtain that $\|\Phi_2\| \leq \|\Phi_{21}\| + \|\Phi_{22}\|$, where By (38) and Lemma 6, Lemma 5

$$\begin{aligned}\Phi_{21} &= \left(T_n^\top \tilde{F}(T_n \gamma^*) T_n \right)^{-1} \left(T_n^\top \tilde{S}(T_n \gamma^*) - S(\gamma^*) \right), \\ \Phi_{22} &= \left[\left(T_n^\top \tilde{F}(T_n \gamma^*) T_n \right)^{-1} - F^{-1}(\gamma^*) \right] S(\gamma^*).\end{aligned}$$

By (38) and (39),

$$\|\Phi_{21}\| \leq \left\| \left(T_n^\top \tilde{F}(T_n \gamma^*) T_n \right)^{-1} \right\| \left\| T_n^\top \tilde{S}(T_n \gamma^*) - S(\gamma^*) \right\| \leq 2C \cdot o_p(n^{-1/2}) = o_p(n^{-1/2}).$$

To bound $\|\Phi_{22}\|$, note first that by Lemma 5 and Assumption 5,

$$\left\| \left(T_n^\top \tilde{F}(T_n \gamma^*) T_n \right) - F(\gamma^*) \right\| \leq \Psi(\|\gamma^*\|) \bar{\tau}_n = o(n^{-1/2}). \quad (49)$$

Also, by Assumption 4, eigenvalues of $F(\gamma^*)$ belong to interval $[1/(2C), 2C]$, therefore bounded away from zero and infinity. This implies that both $\|(T_n^\top \tilde{F}(T_n \gamma^*) T_n)^{-1}\|$ and $\|F^{-1}(\gamma^*)\|$ are bounded from above by an absolute constant, due to the continuity of the inverse map away from

zero. Therefore,

$$\begin{aligned}
\|\Phi_{22}\| &= \left\| \left(T_n^\top \tilde{F}(T_n \gamma^*) T_n \right)^{-1} \left[T_n^\top \tilde{F}(T_n \gamma^*) T_n - F(\gamma^*) \right] F^{-1}(\gamma^*) S(\gamma^*) \right\| \\
&\leq \left\| \left(T_n^\top \tilde{F}(T_n \gamma^*) T_n \right)^{-1} \right\| \left\| T_n^\top \tilde{F}(T_n \gamma^*) T_n - F(\gamma^*) \right\| \|F^{-1}(\gamma^*)\| \|S(\gamma^*)\| \\
&= o(n^{-1/2}) \|S(\gamma^*)\|.
\end{aligned}$$

From (12), we have

$$S(\gamma^*) = \frac{1}{n} \sum_{i=1}^n g_i \eta \left(g_i^\top \gamma^* \right) e_i,$$

where $\eta = h'/v$ denotes a scalar function depending on functions h and v , and e_i 's are independent random variables with zero means and variances $v(g_i^\top \gamma^*)$. By Markov inequality, for any $t > 0$,

$$\mathbb{P}(\|S(\gamma^*)\| > t) \leq t^{-2} \mathbb{E} \|S(\gamma^*)\|^2 = t^{-2} \frac{1}{n^2} \sum_{i=1}^n \|g_i\|^2 \eta^2(g_i^\top \gamma^*) v(g_i^\top \gamma^*).$$

Note that $\|g_i\| \leq C$ by Assumption 3. In particular, $\|g_i^\top \gamma^*\| \leq C \|\gamma^*\|$, and therefore $|\eta^2(g_i^\top \gamma^*) v(g_i^\top \gamma^*)|$ are uniformly bounded over $1 \leq i \leq n$ because $\eta^2 v$ is a smooth function. This implies

$$\mathbb{P}(\|S(\gamma^*)\| > t) = O(t^{-2} n^{-1}).$$

Choosing $t = O(1)$, we obtain that $\|S(\gamma^*)\| = O_p(1)$. This implies $\|\Phi_{22}\| = o_p(n^{-1/2})$ and the proof is complete. \square

The following Linderberg-Feller Central Limit Theorem is needed for proving Theorem 3.

Lemma 11 (Lindeberg-Feller Central Limit Theorem from Lindeberg [1922]). *For each positive integer n , let X_{nj} , $j = 1, 2, \dots, n$, be independent random variables with $\mathbb{E}[X_{nj}] = 0$ and $\mathbb{E}[X_{nj}^2] = \sigma_{nj}^2 < \infty$. Denote $B_n^2 = \sum_{j=1}^n \sigma_{nj}^2$ and assume that for each $\varepsilon > 0$,*

$$\lim_{n \rightarrow \infty} \frac{1}{B_n^2} \sum_{j=1}^n \mathbb{E} [X_{nj}^2 I \{|X_{nj}| > \varepsilon B_n\}] = 0.$$

Then

$$\frac{1}{B_n} \sum_{j=1}^n X_{nj} \rightarrow N(0, 1),$$

where the convergence is in distribution.

Proof of Theorem 3. We fix a unit vector $z \in \mathbb{R}^{p+K-r}$ and derive the asymptotic distribution for the scalar random variable $z^\top (T_n^{-1} \hat{\gamma} - \gamma^*)$; the claims in (20), (22), and (24) will follow from specific choices of z . By Lemma 10, we have

$$z^\top (T_n^{-1} \hat{\gamma} - \gamma^*) = z^\top F^{-1}(\gamma^*) S(\gamma^*) + o_p(n^{-1/2}).$$

Multiplying both sides of this equation with a normalizing factor $\sqrt{n}(z^\top F^{-1}(\gamma^*) z)^{-1/2}$, which is

of order $O(n^{1/2})$ by Assumption 4, we obtain

$$\frac{\sqrt{n}z^\top(T_n^{-1}\hat{\gamma} - \gamma^*)}{(z^\top F^{-1}(\gamma^*)z)^{1/2}} = \frac{n^{-1/2} \sum_{i=1}^n z^\top F^{-1}(\gamma^*) g_i \eta(g_i^\top \gamma^*) e_i}{(z^\top F^{-1}(\gamma^*)z)^{1/2}} + o_p(1),$$

where $\eta = h'/v : \mathbb{R} \rightarrow \mathbb{R}$ is a scalar function. We will prove the asymptotic normality of the first term on the right-hand side of the above equation by verifying the Lindeberg conditions in Lemma 11. Denote

$$\bar{e}_i := z^\top F^{-1}(\gamma^*) g_i \eta(g_i^\top \gamma^*) e_i.$$

It is straightforward that $\mathbb{E}[\bar{e}_i] = 0$ and $\mathbb{E}[\bar{e}_i^2] < \infty$ because g_i 's are bounded by Assumption 3. By (13), the sum of variances of \bar{e}_i are

$$B_n^2 = \sum_{i=1}^n \mathbb{E}[\bar{e}_i^2] = \sum_{i=1}^n z^\top F^{-1}(\gamma^*) g_i g_i^\top \frac{(h'(g_i^\top \gamma^*))^2}{v(g_i^\top \gamma^*)} F^{-1}(\gamma^*) z = n \left(z^\top F_n^{-1}(\gamma^*) z \right).$$

It remains to verify the tail control condition, that is, to show that for each $\varepsilon > 0$,

$$\Phi := \frac{1}{B_n^2} \sum_{i=1}^n \mathbb{E}[\bar{e}_i^2 I\{|\bar{e}_i| > \varepsilon B_n\}] \rightarrow 0.$$

Note that $B_n^2 \geq C^{-1}n$ by Assumption 4. Therefore,

$$\begin{aligned} \Phi &\leq \frac{1}{B_n^2} \sum_{i=1}^n \mathbb{E} \left[|\bar{e}_i|^2 I\{|\bar{e}_i| > \varepsilon C^{-1/2} n^{1/2}\} \right] \\ &= \frac{1}{B_n^2} \sum_{i=1}^n \mathbb{E} \left[|\bar{e}_i|^\xi \left(|\bar{e}_i|^{2-\xi} I\{|\bar{e}_i| > 0\} \right) I\{|\bar{e}_i| > \varepsilon C^{-1/2} n^{1/2}\} \right] \\ &\leq \frac{1}{B_n^2} \sum_{i=1}^n \mathbb{E} \left[|\bar{e}_i|^\xi (\varepsilon^{-1} C^{1/2} n^{-1/2})^{\xi-2} \right] \\ &\leq \varepsilon^{2-\xi} C^{(\xi-2)/2} n^{-(\xi-2)/2} \left(z^\top F^{-1}(\gamma^*) z \right)^{-1} \max_{1 \leq i \leq n} \mathbb{E} |\bar{e}_i|^\xi. \end{aligned}$$

To bound $\max_{1 \leq i \leq n} \mathbb{E} |\bar{e}_i|^\xi$, note that the coefficient $z^\top F^{-1}(\gamma^*) g_i \eta(g_i^\top \gamma^*)$ in the definition of \bar{e}_i is uniformly bounded over $1 \leq i \leq n$ because $\|F^{-1}(\gamma^*)\|$ is bounded by Assumption 4, $\|g_i\| \leq C$ by Assumption 3, and $\eta(g_i^\top \gamma^*)$ is bounded by the continuity of η and the fact that $\|g_i^\top \gamma^*\| \leq C\|\gamma^*\|$. Therefore, by Assumption 6,

$$\max_{1 \leq i \leq n} \mathbb{E} |\bar{e}_i|^\xi = O \left(\max_{1 \leq i \leq n} \mathbb{E} |e_i|^\xi \right) = O(1).$$

This implies $\Phi = O(n^{-(\xi-2)/2})$, and the tail control condition is proved. Therefore, by the Lemma 11,

$$\frac{\sqrt{n}z^\top(T_n^{-1}\hat{\gamma} - \gamma^*)}{(z^\top F^{-1}(\gamma^*)z)^{1/2}} \rightarrow \mathcal{N}(0, 1). \quad (50)$$

Finally, we can replace the denominator of the left-hand side of (50) with the approximation $(v^\top(T_n^\top \tilde{F}(\hat{\gamma})T_n)^{-1}v)^{1/2}$, because of (49) and the fact that $F^{-1}(\gamma^*)$ is bounded from below by

Assumption 4. We conclude

$$\frac{\sqrt{n}z^\top(T_n^{-1}\hat{\gamma} - \gamma^*)}{\left(z^\top \left(T_n^\top \tilde{F}(\hat{\gamma})T_n\right)^{-1} z\right)^{1/2}} \rightarrow \mathcal{N}(0, 1). \quad (51)$$

We now proceed to prove that (20), (22), and (24) are consequences of (51) with proper choices of z . Regarding (24), we choose

$$z_{1:r} = \frac{n^{-1}Z_{1:r}^\top \hat{\mathcal{P}}_R XGu}{\|n^{-1}Z_{1:r}^\top \hat{\mathcal{P}}_R XGu\|}, \quad z_{(r+1):(K+p-r)} = 0.$$

For this choice to be valid, we need to check that the denominator in the formula of $z_{1:r}$ is not zero. Indeed, by condition (21),

$$\begin{aligned} n^{-1} \|Z_{1:r}^\top \hat{\mathcal{P}}_R XGu\| &\geq n^{-1} \|Z_{1:r}^\top XGu\| - n^{-1} \|Z_{1:r}^\top (\hat{\mathcal{P}}_R - \mathcal{P}_R) XGu\| \\ &\geq c - n^{-1} \|Z_{1:r}^\top\| \|\hat{\mathcal{P}}_R - \mathcal{P}_R\| \|XGu\| \\ &= c - n^{-1/2} \|XGu\| \|\hat{\mathcal{P}}_R - \mathcal{P}_R\| \\ &= c - \left(u^\top G \left(X^\top X/n\right) Gu\right)^{1/2} \|\hat{\mathcal{P}}_R - \mathcal{P}_R\| \\ &= c - \left(u^\top Gu\right)^{1/2} \|\hat{\mathcal{P}}_R - \mathcal{P}_R\| \\ &\geq c - C^{1/2} C_2 \bar{\tau}_n \\ &> c/2. \end{aligned}$$

With this choice of z , (51) reduces to

$$\frac{\sqrt{n}v_{1:r}^\top \left(\left(\tilde{Z}_{1:r}^\top Z_{1:r}/n\right)^{-1} \hat{\gamma}_{1:r} - \gamma_{1:r}\right)}{\left(v_{1:r}^\top \left(\tilde{Z}_{1:r}^\top Z_{1:r}/n\right)^{-1} \tilde{F}_1^{-1}(\hat{\gamma}) \left(Z_{1:r}^\top \tilde{Z}_{1:r}/n\right)^{-1} v_{1:r}\right)^{1/2}} \rightarrow \mathcal{N}(0, 1).$$

From (9), the above expression is simplified to

$$\frac{\sqrt{n}u^\top \left(\hat{\theta} - n^{-1}G^\top X^\top \hat{\mathcal{P}}_R Z_{1:r} \gamma_{1:r}\right)}{\left(u^\top GX^\top \tilde{Z}_{1:r} \tilde{F}_1^{-1}(\hat{\gamma}) \tilde{Z}_{1:r}^\top XGu\right)^{1/2}} \rightarrow \mathcal{N}(0, 1),$$

and (24) is proved.

Next, we prove (22) by choosing z such that

$$z_{1:r} = 0, \quad z_{(r+1):p} = \frac{n^{-1}Z_{(r+1):p}^\top \hat{\mathcal{P}}_R XGu}{\|n^{-1}Z_{(r+1):p}^\top \hat{\mathcal{P}}_R XGu\|}, \quad z_{(p+1):(K+p-r)} = 0.$$

The denominator of the formula for $z_{(r+1):p}$ is non-zero because by condition (21),

$$n^{-1} \left\| Z_{(r+1):p}^T \hat{\mathcal{P}}_C X G u \right\| \geq c - C^{1/2} C_2 \bar{\tau}_n > c/2.$$

With this choice of z , (51) is equivalent to

$$\frac{\sqrt{n} v_{(r+1):p}^\top \left(\left(\tilde{Z}_{(r+1):p}^\top Z_{(r+1):p}/n \right)^{-1} \hat{\gamma}_{(r+1):p} - \gamma_{(r+1):p} \right)}{\left(v_{(r+1):p}^\top \left(\tilde{Z}_{(r+1):p}^\top Z_{(r+1):p}/n \right)^{-1} \tilde{F}_1^{-1}(\hat{\gamma}) \left(Z_{(r+1):p}^\top \tilde{Z}_{(r+1):p}/n \right)^{-1} v_{(r+1):p} \right)^{1/2}} \rightarrow \mathcal{N}(0, 1).$$

From (10), the above expression is simplified to

$$\frac{\sqrt{n} u^\top \left(\hat{\beta} - n^{-1} G^\top X^\top \hat{\mathcal{P}}_C Z_{(r+1):p} \gamma_{(r+1):p} \right)}{\left(u^\top G X^\top \tilde{Z}_{(r+1):p} \tilde{F}_2^{-1}(\hat{\gamma}) \tilde{Z}_{(r+1):p}^\top X G u \right)^{1/2}} \rightarrow \mathcal{N}(0, 1),$$

and (22) is proved.

Finally, we show (20). For any unit vector $u \in \mathbb{R}^{K-r}$, choose

$$z_{1:p} = 0, \quad z_{(p+1):(p+K-r)} = \frac{\left(\tilde{W}_{(r+1):K}^\top W_{(r+1):K}/n \right) \tilde{F}_3^{1/2}(\hat{\gamma}) u}{\left\| \left(\tilde{W}_{(r+1):K}^\top W_{(r+1):K}/n \right) \tilde{F}_3^{1/2}(\hat{\gamma}) u \right\|}.$$

Then by a direct calculation,

$$z^\top \left(T_n^\top \tilde{F}(\hat{\gamma}) T_n \right)^{-1} z = \frac{1}{\left\| \left(\tilde{W}_{(r+1):K}^\top W_{(r+1):K}/n \right) \tilde{F}_3^{1/2}(\hat{\gamma}) u \right\|^2},$$

while $\sqrt{n} z^\top (T_n^{-1} \hat{\gamma} - \gamma^*)$ equals

$$\begin{aligned} & \sqrt{n} z_{(p+1):(p+K-r)}^\top \left(\left(\tilde{W}_{(r+1):K}^\top W_{(r+1):K}/n \right)^{-1} \hat{\gamma}_{(p+1):(p+K-r)} - \gamma_{(p+1):(p+K-r)}^* \right) \\ &= \frac{\sqrt{n} u^\top \tilde{F}_3^{-1/2}(\hat{\gamma}) \left(\hat{\gamma}_{(p+1):(p+K-r)} - \left(\tilde{W}_{(r+1):K}^\top W_{(r+1):K}/n \right) \gamma_{(p+1):(p+K-r)}^* \right)}{\left\| \left(\tilde{W}_{(r+1):K}^\top W_{(r+1):K}/n \right) \tilde{F}_3^{1/2}(\hat{\gamma}) u \right\|}. \end{aligned}$$

Therefore, (51) reduces to

$$\sqrt{n} u^\top \tilde{F}_3^{-1/2}(\hat{\gamma}) J(\hat{\gamma}, \tilde{W}) \rightarrow \mathcal{N}(0, 1),$$

where

$$J(\hat{\gamma}, \tilde{W}) = \hat{\gamma} - \left(\tilde{W}_{(r+1):K}^\top W_{(r+1):K}/n \right) \gamma_{(p+1):(p+K-r)}^*.$$

Since unit vector $u \in \mathbb{R}^{K-r}$ is arbitrary, by Cramer-Wold devices,

$$\sqrt{n} \tilde{F}_3^{-1/2}(\hat{\gamma}) J(\hat{\gamma}, \tilde{W}) \rightarrow \mathcal{N}(0, I_{K-r}).$$

By the continuous mapping theorem,

$$nJ(\hat{\gamma}, \tilde{W})^\top \tilde{F}_3^{-1}(\hat{\gamma})J(\hat{\gamma}, \tilde{W}) \rightarrow \chi_{K-r}^2. \quad (52)$$

By the Schur complement formula, $\tilde{F}_3^{-1}(\hat{\gamma})$ equals

$$\frac{1}{n} \left(\tilde{W}_{(r+1):K}^\top \kappa(\hat{\gamma}) \tilde{W}_{(r+1):K} \right) - \frac{1}{n} \left(\tilde{W}_{(r+1):K}^\top \kappa(\hat{\gamma}) \tilde{Z} \right) \left(\tilde{Z}^\top \kappa(\hat{\gamma}) \tilde{Z} \right)^{-1} \left(\tilde{Z}^\top \kappa(\hat{\gamma}) \tilde{W}_{(r+1):K} \right),$$

where

$$\kappa(\hat{\gamma}) = \text{diag} \left((h'(\tilde{g}_i^\top \hat{\gamma}))^2 / v(\tilde{g}_i^\top \hat{\gamma}) \right).$$

Therefore, (52) can be further simplified to

$$n \left(\hat{\alpha} - n^{-1} \tilde{W}_{(r+1):K} \tilde{W}_{(r+1):K}^\top \alpha^* \right)^\top \tilde{O} \left(\hat{\alpha} - n^{-1} \tilde{W}_{(r+1):K} \tilde{W}_{(r+1):K}^\top \alpha^* \right) \rightarrow \chi_{K-r}^2,$$

where $\tilde{O} = n^{-1}(\kappa(\hat{\gamma}) - \kappa(\hat{\gamma}) \tilde{Z} (\tilde{Z}^\top \kappa(\hat{\gamma}) \tilde{Z})^{-1} \tilde{Z}^\top \kappa(\hat{\gamma}))$. The proof is complete. \square

F The Proof of Corollary 2

Proof. A solution to the estimating equation $\tilde{S}(\gamma) = 0$ is a critical point of the likelihood function. It is unique if the likelihood function is concave or, equivalently, if $\partial \tilde{S}(\gamma) / \partial \gamma$ is a negative-definite matrix for any γ . When the link function is natural,

$$\frac{\partial \tilde{S}(\gamma)}{\partial \gamma} = - \sum_{i=1}^n \left(\tilde{Z} \tilde{W}_{(r+1):K} \right)^\top \kappa(\gamma) \left(\tilde{Z} \tilde{W}_{(r+1):K} \right), \quad \text{where } \kappa(\gamma) = \text{diag} \left(\frac{(h'(\tilde{g}_i^\top \gamma))^2}{v(\tilde{g}_i^\top \gamma)} \right)$$

We will show that each summand in the formula of $\partial \tilde{S}(\gamma) / \partial \gamma$ is a positive definite matrix. First, regarding $\kappa(\gamma)$, by the definition of the smooth increasing function h in (2), each diagonal entry of $\kappa(\gamma)$ is positive. Therefore, it remains to show that $\tilde{Z} \tilde{W}_{(r+1):K}$ is of full rank. Since $\text{span}(\tilde{Z}) = \text{col}(X)$ and $\text{span}(\tilde{W}_{(r+1):K}) = \hat{\mathcal{N}}$, this is equivalent to $\text{col}(X) \cap \hat{\mathcal{N}} = 0$. This identity holds if we prove that for any unit vector $u \in \text{col}(X)$, the projection of u onto $\hat{\mathcal{N}}$ has norm strictly less than one. To show that, we write $u = n^{-1/2} Zx$ for some $x \in \mathbb{R}^p$ with $\|x\| = 1$ and note that the projection onto $\hat{\mathcal{N}}$ is $\hat{\mathcal{P}}_N$. By Proposition 1, the singular value decomposition in (6), and Assumption 5,

$$\begin{aligned} \left\| \hat{\mathcal{P}}_N u \right\| &\leq \left\| \mathcal{P}_N u \right\| + \left\| \left(\hat{\mathcal{P}}_N - \mathcal{P}_N \right) u \right\| \\ &\leq n^{-1/2} \left\| \mathcal{P}_N Z_{1:r} x_{1:r} \right\| + n^{-1/2} \left\| \mathcal{P}_N Z_{(r+1):K} x_{(r+1):K} \right\| + C_1 \bar{\tau}_n \\ &= n^{-1} \left\| W_{(r+1):K}^\top Z_{1:r} x_{1:r} \right\| + n^{-1} \left\| W_{(r+1):K}^\top Z_{(r+1):K} x_{(r+1):K} \right\| + C_1 \bar{\tau}_n \\ &= n^{-1} \left\| W_{(r+1):K}^\top Z_{(r+1):K} x_{(r+1):K} \right\| + C_1 \bar{\tau}_n \\ &\leq n^{-1} \left\| W_{(r+1):K}^\top Z_{(r+1):K} \right\| \left\| x_{(r+1):K} \right\| + C_1 \bar{\tau}_n \\ &\leq \sigma_{r+1} \|x\| + C_1 \bar{\tau}_n < 1, \end{aligned}$$

for sufficiently large n . The proof is complete. \square